1-30-2012

Second Generation Data-Logging System for Long-Duration Field Measurement of Vibration Exposure and Grip Force

Robert H. Knapp III
University of Connecticut - Storrs, robert.h.knapp@gmail.com

Second Generation Data-Logging System for Long-Duration Field Measurement of Vibration Exposure and Grip Force

Robert Holland Knapp III

B.A., University of Connecticut, Biomedical Engineering, December 2009

A Thesis

Submitted in Partial Fulfillment of the

Requirements for the Degree of

Master of Science

at the

University of Connecticut

2012

APPROVAL PAGE

Master of Science Thesis

Second Generation Data-Logging System for Long-Duration Field Measurement of Vibration Exposure and Grip Force

Presented By

Robert Holland Knapp III, B.S.

Major Advisor_____

Dr. Donald R. Peterson

Associate Advisor_____

Dr. Anthony J. Brammer

Associate Advisor_____

Dr. Martin G. Cherniack

University of Connecticut

2012

Acknowledgements

I would like to thank Dr. Donald Peterson, Dr. Martin Cherniack, and Dr. Anthony Brammer for funding and supporting the research conducted for completion of this thesis. I would also like to thank Dr. Anthony Brammer for his advice concerning the electronics design and performance testing. Also, his suggestions for noise reductions and design of the analog front end for the accelerometer sensors were greatly appreciated.

The students and staff of the Biodynamics Laboratory all provided valuable support to complete this project. Eric Bernstein helped at every stage of the device development, giving advice on how to fix any problem encountered in making his device. Takafumi Asaki helped with any Labview programming problems encountered, providing advanced knowledge in the field of vibration equipment as well as background and setup of testing devices. Shane Tornifoglio helped create the analog front end for the force sensors and helped with circuitry issues. Also, all the University of Hartford undergraduate student volunteers who helped conduct the tests of the system-sensor performance. Thanks to Marek Wartenberg and Christopher Larson for their help designing and programming parts of the Secured Digital card code and analog to digital converter code.

Finally, I would like to thank my parents for encouraging me through out the project. Their support and interest in my work increased my productivity as well as learning ability while creating this device.

Abstract

Millions of United States workers are exposed to vibration at their job, whether it is from a power tool that causes hand and arm vibration or from heavy machinery that exposes them to whole body vibrations. These vibrations are known to result in physical disorders such as Hand-Arm Vibration Syndrome, which can be debilitating to the point where workers can no longer do their job effectively. Research groups have taken an interest in finding what vibration characteristics are most harmful and choose to record vibration information using data-logging devices. Often, many devices, whether they are commercial or custom-built devices, use frequency weightings and full day estimations to measure vibration exposure, in which data can be lost due to pre-software filtering and short measurement durations.

Described in this thesis is a high-end data-logging device that was created as a significant improvement to the vibration data-logging devices that have typically been used in past research. Using surface mount components on a custom-designed printed circuit board, it was possible to create a portable device that captured full vibration waveforms over multiple channels: 8 channels of force and 8 channels of acceleration. In this device, signals are anti-alias filtered, sampled, converted, and stored to a solid state memory device over the course of an entire workday (i.e., greater than or equal to 8 hours). The device created in this thesis has met specifications for resolution of force and accelerations channels that are 10- and 14-bits, respectively. Sampling rate specifications were also met, with force channels being sampled at 908 Hz and acceleration channels sampled at 5000 Hz each. A final robust dynamic range of 1 to 1000 m/s^2 peak-to-peak was achieved for the acceleration channels and the specification for the device to last a

minimum of 8 hours was also achieved to allow for data capture of raw signals for over 9 hours.

Table of Contents

Table of Figures

Table of Tables

1 Introduction

1.1 Background

In the United States 8-10 million workers are exposed to some sort of vibration at their job [1]. Some jobs expose workers to more vibration than others such as ones involving heavy machinery (whole body vibration) and power tools (hand-arm vibration). Hand-arm vibrations can result in serious health issues due to hand-arm vibration syndrome (HAVS): symptoms include joint stiffness, digital vasospasms (vibration white fingers), numbness and tingling, as well as pain. In the UK an estimated 300,000 working days are lost annually due to HAVS [2]. Due to the debilitating nature of HAVS it has become an area of interest for research groups to find what aspect of the vibration causes the disorder. There is no current cure for the syndrome; therefore, finding the cause may be useful in creating preventative measures, such as vibration filtering gloves or a better estimate for a safe amount of vibration exposure.

HAVS involves disorders related to vascular, neurological, bone and joint, and muscular aspects of the body. Secondary Raynaud's phenomenon is a neurovascular response: in the case of HAVS the response is due to vibration. From HAVS, vascular disorders include vasospasms that result in blood occlusion from fingers and parts of the hand. The damage causing the vascular disorders is done by vibration but the attacks of pain can also be brought on by cold temperatures. Neurological disorders include the feeling of numbness and tingling even without vibratory provocation. Carpal tunnel syndrome which also causes loss of feeling in the hands and loss of grip force occurs more frequently in vibration exposed workers [3]. Damage to the lunate bone of the wrist is common and is thought to occur due to reduced blood supply to the bone during

vibration along with compressive microfractures [4]. There is chronic loss of tool grip during vibration exposure and grip forces are commonly measured in conjunction with accelerations [5]. In addition, there are others reported disorders that are related to hand and arm, such as hearing loss, back pain, and abdominal injuries have been reported [4].

Due to the fact that HAVS is a multi-system disorder, tests on the vascular, neurological, and musculoskeletal aspects of the hand are performed. Neurological tests include nerve conduction, current perception thresholds, vibration perception thresholds, thermal perception thresholds, two-point discrimination, grip strength, as well as others. A widely used vascular test is the finger skin temperature (FST). The test is performed by submerging the hand in cold water at a standardized temperature for 5 minutes. The hand is then removed and the FST is monitored to find how long it takes for it to return to normal. Lengthened re-warming time indicates vasospasms that are known to occur in HAVS. Most of these tests can help describe the symptoms caused by the syndrome, but are unable to describe what vibration parameters caused it. To get a better idea of what types of vibration the workers are exposed to at their job, devices have been made to be worn by the workers during their normal work day to measure vibration exposure. Previous vibration data-logging devices from research laboratories may be helpful in estimating the risk of obtaining HAVS from certain tools but they may not be able to capture data as fully as they can now. Significant advances in technology allow a newer device to be made to capture a larger range of vibration frequencies, larger magnitudes of vibration, record whole vibration signals (as opposed to weighted averages), allow for more acceleration and force sensor connections, allow for more data storage, record for a

full day, and is comparable in size to other portable data-logging devices. The device described will allow for better data analysis of vibration signals.

Many devices used in industry are for hygienic purposes to allow workers to know how much vibration they are being exposed to and when, in the future, they should stop using a tool. Most devices implement measurement procedures described in standards. The first is described in ISO-5349-1, namely a graph containing weight values for different frequencies of vibration. Many commercial devices use these weightings and apply it to the raw vibration exposure. The standard states that vibrations below 8 Hz and above 1000 Hz "are not agreed" and should not be taken into consideration for analysis. These weightings may not be appropriate for monitoring vibration white finger [6], which may become a serious condition obtained from exposure to vibration. Another estimation technique used is the daily vibration exposure, which is known as A(8), which is the eight hour energy equivalent vibration exposure value defined in ISO 5349. This value estimates how much vibration exposure a person will get in one eight hour work day judging by data collected for all or a fraction of the day. Other values can be calculated as well, such as A(4), or A(2), in which both of these values correspond to the amount of vibration exposure a worker will be subjected to in 4 hours and 2 hours, respectively.

The standards assume exposure is related solely to the acceleration at a surface in contact with the hand. Most vibration standards do not include grip force measurements; one exception is ISO-10819. The transmissibility of the vibration may be important. It could indicate how much vibration will be transferred from the tool to the surface of the hand of the subject. It also has been shown that grip force can cause changes in the

amount of transmissibility of a tool [7]. Most standards do not take grip force of the tool into consideration and more research needs to be done on the topic.

1.2 Previous Devices

Data logging devices were devised 50 years ago when digital devices were a thing of the future. Holter et al. developed a datalogger, called an electrocardiocorder, in 1961 to record heart rhythms over an extended period of time [8]. It was one of the first portable dataloggers. It was made to be held in a pocket or handbag with leads running to it hidden under the subject's shirt. Leads then connected to the chest measuring electrocardiogram signals. Signals were recorded to magnetic tape that was capable of holding up to 10 hours of data. The power supply of the device allowed for up to 100 hours of data capture. A predecessor of this device was the radioelectrocardiograph. It would transmit data signals from the subject to a briefcase kept within the vicinity of the subject through radio frequencies [8].

1.2.1 Commercial Devices

Available commercial vibration dataloggers are mainly designed for limited industrial purposes; however, they are used by some research groups to attempt to collect detailed information. These devices employ low number of acceleration sensor inputs and are useful for monitoring workers vibration exposure for hygienic purposes since the user only has to be connected to a few sensors. Most of the commercial devices take measurements and apply a frequency weighting of the RMS acceleration, created to estimate what vibration frequencies are more likely to cause damage. These weightings are defined in ISO-5349-1 (2001) and are used as a standard for vibration exposure. The standard does not incorporate hand-tool forces.

Marketed devices do not possess the defining specifications of the datalogger described in this thesis. A representative device made by Larson Davis, Model HVM 100, captures vibration signals with a frequency range from 0.4 Hz up to 1250 Hz. It allows for three acceleration sensor inputs, measuring X, Y, and Z directions of vibration. The HVM 100 uses the A(8) exposure metric, where the amount of vibration exposure from a tool is estimated for 8 hours of use without necessarily having the subject wear the device all day. The device allows the user to apply different weighted filters to the vibration signal as well. Vibration exposure is displayed on a built in screen or can be outputted to a computer.

Another commercial developer of vibration data-logging devices is Brüel & Kjær, which has marketed the product, Human Vibration Analyzer Type 4447. Similar to the HVM 100, the 4447 has three acceleration sensor inputs and allows for different weighted averages to be applied to vibration signals. One drawback to the device is that it can only be used for a maximum of 4 hours. This is justified as being sufficient when using an A(8) estimation of vibration exposure And when 4 hours is sufficient in characterizing the patterns of exposure.

1.2.2 Research Devices

Customized, high-end, laboratory devices are capable of collecting data longer than an entire day with high resolution and frequency ranges exceeding ISO standards. The drawback is that these devices are not portable and cannot be used in the field for full work day measurements due to their bulkiness as these devices contain large conversion boxes and laptop computers. For data collection in the field, a smaller battery- powered

device is desired; however, smaller portable devices come with reduced capabilities due to the lack of battery life and storage capacity.

Some laboratory groups prefer not to use commercial devices for their research because custom specifications are needed. Custom specifications usually end up containing many trade offs. For example, if a large number of channels are required, sampling rates must be chosen accordingly due to restrictions on data storage space. If high resolution is required, maximum and minimum voltage readings must be considered, but a larger range of voltages reduces the resolution of the system if the bit count is constant. Also, if long battery life is required, the size of the device needs to be considered to allow space for the appropriate number of batteries. User interfaces can also draw large amounts of current from the batteries, so whether or not to include an interface is an important design consideration.

A research group in India designed a data logging device used to measure temperature and humidity. The device incorporated eight input channels sampled with 10 bit analog to digital (A/D) resolution and had the ability to send the data to the user's phone using a short message service. The device has a user display and is able to capture data from 30 seconds to 99 minutes, allowing up to 1 GB of storage on a MicroSD card [9]. A device as such is not adequate if a full day of analysis is required.

A research group in Beijing, China created a general purpose data-logging device to accommodate up to 32 analog channels and sampled signals up to 10 KHz per channel. Although the sampling rate is high the trade off is that data collection time is only 3 minutes due to the lack of external data storage space. The device allowed for different resolutions of data capture: 6 bit, 12 bit, and 14 bit [10].

High-resolution long-lasting data loggers have been made to measure seismic activity on submarines as well. Since these devices have high resolution (24 bits), each sample must be represented by three bytes. Since this device is meant to capture data for long periods of time, it will be storing massive amounts of data if sampling at rates as high as the previous datalogger described. This device has sacrificed its sampling rate to one hundredth that of the previous dataloggers sampling rate, namely 100 Hz per channel, which was acceptable for its purpose [11].

Due to the differences in each research group goals, there is no perfect datalogger for every purpose. Sensors for different purposes, temperature, acceleration, force, humidity, etc. have different requirements for the front end circuitry (analog filtering, amplification, etc.) of the datalogger. Different input impedances are needed as well as different gains. In the three previous examples, user friendly data loggers have been described with the capability to send messages to the user's phone. These devices cannot capture data for full work days and their resolution is quite average. High sampling speeds over many channels was described; the problem is data capture time is miniscule. Very high resolution data capture was also described with long capture times; however, the sampling rate had to be low to allow this. Thus, for research purposes, a custom datalogger is necessary.

1.2.3 Previous Generations

1.2.3.1 First Generation

A vibration datalogger was created by Peterson et al. of the UConn Biodynamics Laboratory called the Vibration Exposure Monitor (VEM) system and is shown in Figure 1 [12]. It is used to capture vibration data from a full day of work. The device captured

data from two sensors, a uni-axial accelerometer (Model 352C22, PCB Piezotronics, Depew, NY) and a force sensitive resistor (Model 400, Interlink Electronics, Camarillo, CA), mounted on the palm (shown in Figure 1 below). Unlike many commercial devices, the force measurement was recorded in conjunction with the acceleration. This allows insight into how well the subjects hand is coupled to the tool being used. The device would sample at 3 kHz for 15 seconds every minute. When finished sampling, the device would switch to a low power computational mode, during this time it would calculate weighted and unweighted values including root mean square (RMS), root mean quad (RMQ), and root mean oct (RMO) as well as maximum and minimum grip force from the force sensitive resistor. The device was powered using three 9 volts batteries, allowing a rated capacity of 570 mAh. The low power mode allowed the device to draw less than 250 μA as opposed to the 150 mA during sampling time. Since the device was in low power mode most of the day it could last much longer, allowing a full day of data capture. The data collected were stored in a volatile memory location, which means that if power is lost before data are retrieved, then the data would be lost. To allow the device to last even longer after data collection was finished, the device went into a sleep mode to significantly reduce power consumption and maintain stored data until retrieval by the user. Data transfer from the device was accomplished using an RS-232 serial port [12]. Some other drawbacks to the device resulted from its volatile data storage structure. Since the power had to be turned off before the data were removed, new batteries had to be used every time data capture was required. Also, a laptop computer had to be brought into the field to retrieve the data from the device soon after capture was finished.

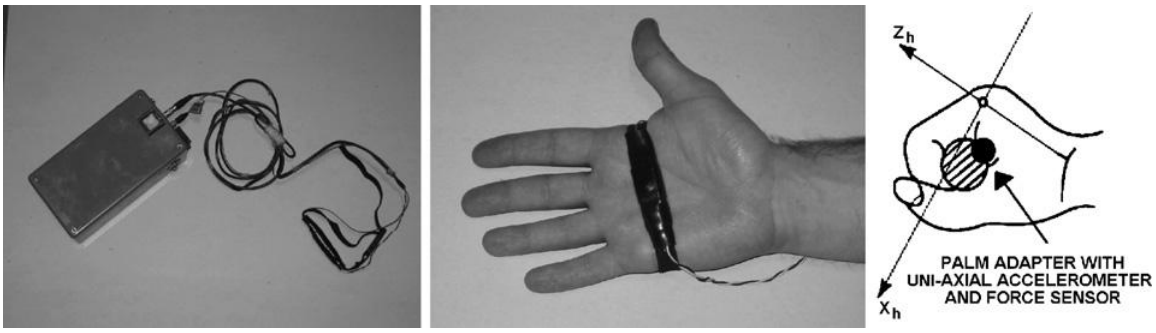

Figure 1: Vibration exposure monitor (left), palm adaptor with accelerometer and force sensitive resistor (middle), and an example of the palm adapter in use (right). Figure from Peterson et. al. [12]

The device had several aspects to be improved. Due to the lack of battery capacity and storage space, the device was limited to 15 second windows of data capture for each minute of sampling. This means only one quarter of the vibration data is actually measured through out the workday. Some commercial devices use full day estimations of vibration from only a few hours of data capture; the VEM system estimates a full minute's vibration from a fraction of a minute, where the device is capturing for 15 seconds and assumes the other 45 seconds are similar.

As explained earlier ISO standards use frequency weighted filters. There was confusion with the VEM system concerning weighted and unweighted values. Since the weighted values are calculated from the unweighted values using a perfect filter, it should never be seen that the weighted values are higher than the unweighted, especially given the nature of the ISO filter. This applies to the values of the weighted and unweighted RMS, RMQ, and RMO. However, in several daylong data captures, weighted values were found to be higher than the unweighted values. It was determined that due to component tolerances and the ±2 dB gain tolerance specified by ISO 5349, it is possible to capture weighted values that are slightly higher than unweighted values. To correct

this apparent inconsistency, the raw data could be digitally filtered, but since the VEM did not store raw data the values could not be corrected in this manner. The development of larger storage capacities over the last decade that are non-volatile allows for full vibration waveforms to be captured rather than signal metrics, which this solves the issues with the first generation VEM system (see Section 1.2.3.2). This would also remove the need to perform any calculations during data capture, since they can all be performed during in software data analysis.

1.2.3.2 Newer Generation Datalogger

A newer generation datalogger was created, which embodied significant improvements over the VEM system, and was designed for electrogoniometry instead of force and vibration (see Figure 2). A changeable front end circuit was constructed, making it capable of interfacing with a vibration front end to record acceleration and force. It increased the number of channels from 2 to 10 electrogoniometer sensor inputs. The device converted data using a 12 bit resolution A/D converter on board the microcontroller. Data were captured continuously and saved to secured digital (SD) cards in a file allocation table (FAT) 32 format (see Section 2.5). FAT32 format allows easy file removal from SD cards since the data would be in the form of a notepad file. Unlike the previous device, since SD cards were used, the device could lose power and not lose data. The device was designed to sense low power and closes the current file on the SD card. The device allowed for a serial connection to a computer enabling it to communicate with the processor, which is used for manual insertion of calibration values to the SD card. An event switch was implemented as well; it would place a marker in the data when pressed. The event switch is useful for calibration purposes and for data

analysis to mark when something directed by the researcher is occurring. A parallel port was also incorporated into the box; allowing the analog front ends raw signals to be displayed on an oscilloscope.

Figure 2: Electrogoniometer data logging device

In general, the specifications of the box included a sampling rate of up to 4 kHz, 12-bit A/D resolution across a voltage range of 0.5 to 4.5 volts with a virtual ground set at 2.5 volts (allowing ±2 volts swing), and 10 sensor input channels, where he individual channel noise of the box fluctuated between 10 mV and 20 mV [13].

A few drawbacks to the design were experienced. The sampling frequency was originally specified to be 4 kHz per channel for vibration measurements. Although this was reached, it was lowered for the electrogoniometer front end. A battery recharge circuit was also implemented into the board to allow easy battery charging by not having to remove the batteries but, although the recharge circuit worked in prototyping the device, it did not work in the final design. Another drawback with this device was that the sensor connections were directly soldered to the printed circuit board, which made the

printed circuit board difficult to remove for component replacement or debugging purposes. Also, the battery pack and the SD cards were very difficult to remove from the device for recharging and data analysis. Finally, large voltage spikes were seen in this device and later found to occur whenever the microcontroller was writing to the SD card. The large spikes added a known noise to the data collected in the field and could not be removed, only suppressed to an acceptable level.

This generation of datalogger (here after called the Electro Goniometer Data Logger; EGDL) improved upon the original VEM system, due to changes in its circuitry as well as many advances in technology (e.g. SD memory). Since the creation of this device, SD technology has improved further to allow data storage for multi-channel full waveforms at high sampling rates for entire work days and the use of surface mount components would allow for the device to be reduced in size.

1.3 Objectives

Just like the creation of the EGDL system improved on the VEM system, a newer data-logging device was proposed to improve on the EGDL system. In this section, the limitations of the previous data-logging systems are briefly reviewed in order to highlight aspects which were targeted for improvements in the new data-logging system developed in this thesis.

When the VEM system was developed, solid-state memory devices were unable to be utilized and this was corrected in the next generation by using SD card technology. In general solid-state memory technology has been improved to allow for larger amounts of data storage as well as faster write speeds. Slow write speeds in the EGDL caused sampling rates to be decreased due to data write collisions. With faster write speeds the

new device can sample at higher speeds with more channels. The increase in channels and in sampling rate, and capturing for the same amount of time, results in larger amounts of data; therefore, larger capacity SD cards are required as well.

Higher sampling rates are desired by research groups in order to improve upon the resolution of captured signals in the time domain for extremely detailed data analysis. Vibration exposure standards described by ISO 5349 are only specified up to 1.25 kHz; therefore, with higher sampling rates vibration frequencies above the standard can be investigated as well. Oversampling is always desired as long as it is feasible and that adequate data analysis is able to be performed on large data sets.

The commercially available devices are able to record full vibration waveforms but none have the capability to record over long durations (i.e. 8 hrs or a complete working day).The next generation data logger needed to be able to reliably capture raw vibration waveforms for long durations. The increase in sensor inputs from the original VEM system allows for more areas of interest to be measured. A new vibration datalogger would make further improvements by incorporating a force sensor for each accelerometer, in order to measure grip force at each point that acceleration is being measured. These additional channels allow for simultaneous measurements on both hands or for tool and hand measurements for transmissibility properties during tool use.

The VEM had a digital resolution of 12 bits, which was matched by the EGDL, but larger dynamic ranges of acceleration measurements higher resolution was desired. Through the adjustment of the gain of the front end circuit, higher accelerations can be measured but with the increase in range, a decrease in resolution is typical. In order to solve this, an analog to digital converter, with more bits of resolution, is needed. Also,

increasing the range of measurements is helpful in not losing information. Any measurement outside the range of the system is clipped to the maximum possible measurement allowed by the system and if a system does not allow for a high maximum measurement, the data may not give accurate results.

One feature the VEM and the EGDL had in common was the fact that all connections from the board to the outside of the box were soldered. This made it very difficult for debugging purposes as well as component replacement. A new method of connection using plugs to connect from the box to the board would allow for easy removal of the board from the box.

Other aspects of the previous generations of dataloggers do not need to be updated or replaced. For example, the event switch should be implemented in all future boxes and the parallel port connection, to allow instantaneous measurement of the analog output, have been extremely useful throughout past research.

1.4 Previous Work on the Current Device

The digital circuit was constructed before the beginning of this thesis work and included the breadboard design of the microcontroller, the SD card, and the low power circuitry. The initialization of the serial peripheral interface (SPI) ports and the SD card were also previously programmed into a microcontroller and Single Block Write and Read commands were structured as well. The first set of tests at the start of the thesis was to make sure the SD card was being written to and read from properly. A single block of data is 512 bytes and, with larger amounts of data blocks needed, another command called Multiple Block Write needed implementation in the coding.

2 Methods

2.1 Overview

The device described in this thesis is a next-generation datalogger designed to measure human exposure to vibration over long durations. The box allows for 16 sensor inputs, where acceleration and force have either dedicated channels each. The device is started by the user with the push of a button and, after initialization is finished, the device begins converting amplified analog voltages from the connected sensors into digital values. Once a buffer of the digital values is filled, they are stored on a SD card. If the user depresses the power button again, the current file is closed and the circuit is shut off or, if the circuit loses power, the system closes the file to preventing data loss before powering off. The data is retrieved by removing the SD card from the datalogger, on which a data file, in FAT32 format, has been written. Data appears as hexadecimal values that can be split into separate files with respect to channel number via a C# (Microsoft Corporation, Redmond, WA) program. The separate files will contain a list of voltage values for the particular channel and are analyzed using a MATLAB (MathWorks, Natick, MA) program.

The circuit contains 8 different integrated circuits (IC's) with a microcontroller as the master component, which controls data capture rates and the writing of data to the memory. To convert acceleration values from analog to digital, an A/D IC is used and is controlled by the master, while A/D converters built into the microcontroller are used to convert force values. The IC's on the analog front end include operational amplifiers (op amps) which are used as amplifiers and filters for the acceleration and force sensors. Also, the op amps are used as buffers for impedance matching between the sensors and

the A/D converters. Voltage regulator IC's are used to power the circuit, where most of the circuit requires +5 volts except for the SD card, which requires +3.3 volts. To communicate between the microcontroller and the SD card, a voltage level conversion must be performed. This is done using a multiplexer, namely the MAX4619CPE+ (Maxim, Sunnyvale, CA), which takes +5 volts digital signals from the microcontroller and converts them to +3.3 volts digital signals. Another IC is a comparator, which is used in shutting the device off and sensing for a low battery condition (see Section 2.4.3). Finally, an IC is used as a switching regulator.

The force channels are amplified using an inverting amplifier circuit. Since the A/D converters are unable to read negative values, the inverter needs to be powered off a negative voltage. A switching regulator is used that allows for a -5 volt output. Also, the accelerometers have strict requirements for their use, where they need current regulation, and certain minimum voltage. To power the accelerometers, a second battery stack was used to supply the accelerometers with a dedicated +18 volts. The diagram of the data logger circuit is shown in Figure 3 and outlines chip communication. Figure 3 shows that most chips are in direct communication with the microcontroller.

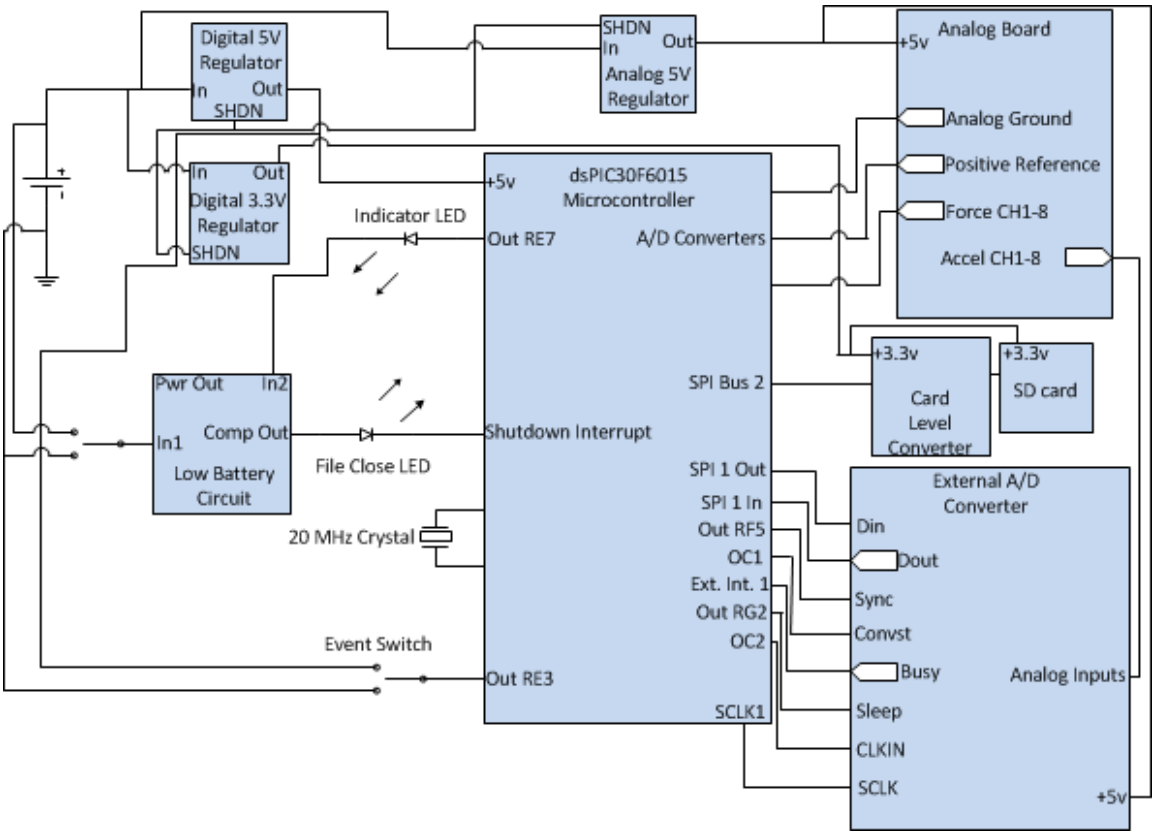

Figure 3: Block diagram of the circuit

2.2 Specifications

The circuit and batteries were required to fit in a project box (see Figure 2) that is appropriate for use in the field and for a subject to wear. The dimensions are 215 mm long by 108 mm wide by 44 mm thick. The force channels were specified to sample voltages of at least 100 Hz per channel. The acceleration channels were specified to sample voltages of at least 5000Hz. Accelerations from 1 m/s^2 up to 1000 m/s^2 peak to peak were specified to be the target range. Forces between 1 lbs. and 100 lbs. were specified to be recorded. Recording times of at least 8 hours were also specified.

2.3 Circuit Functionality

To turn on the device, the user presses the power switch. If running properly the power switch LED will remain lit with a solid color. The linear voltage regulators are always powered by the batteries; however, these chips have a shutdown pin, which controls whether there is output voltage or not. The switch which is toggled by the user creates a voltage at the shutdown pin and causes the chip to output its specified voltage. The shutdown pin voltage is controlled by two sources inputted into an OR gate. This means that this switch can power the shutdown pin, the microcontroller can power the shutdown pin, or both. Therefore, the voltage regulators give power to the microcontroller, which initializes itself and outputs a programmed +5 volts from one of its many input/output (I/O) pins. This voltage is inputted into the OR gate with the battery voltage from the switch (see Section 2.4.3).

2.3.1 Initializations

After power is established and maintained, the microcontroller uses serial peripheral interface buses (SPI) to communicate with the SD card and the external A/D converter. The microcontroller initializes parameters for the SPI and then continues to initialize the SD card. Since multiple SD card types are used, there are different processes for initialization. The microcontroller is able to determine the card type, namely, standard capacity cards (2 GB) and high capacity cards (4-32 GB), and is able to change the initialization accordingly. The main difference between the two cards is the addressing of data sectors, where, in the standard capacity cards the sectors are indexed by byte number and in high capacity cards the sectors are indexed by sector number. In order to calculate

standard capacity sector numbers based on high capacity sector numbers, the location of the sectors must be multiplied by 512, since there are 512 bytes per sector.

Just as the EGDL could sense when power was low and when the power switch was pressed to off, this device does the same. Interrupt flags are initialized to sense a change on the positive edge of the comparator output (see Section 2.3.3).

The A/D converters are initialized next. The acceleration channels are converted using an external IC. Since force channels on the new box are sampled at a much slower rate and need less resolution than the acceleration channels, they are converted using A/D converters on board the microcontroller. Initializing the acceleration channels involves initializing the external A/D converter, where the conversion rate for the external converter is determined by an output compare clock on board the microcontroller, which this must be initialized as well. Force and acceleration A/D converters are initialized at the earliest time possible because it takes time to prepare the output compare conversion clocks. Since the SPI is used in the process of initializing the acceleration A/D converter, the SPI must be initialized beforehand. Also, since the box can be shut off at any time a low power level is detected, interrupts must be initialized early as well. Finally, FAT32 initializations are not needed to initialize the A/D converters and are initialized later in order to give the converters extra time to finish their initializations.

Data storage is in FAT32 file format, which was implemented in the EGDL system as well. When formatting a SD card using a computer, a selection of formats is available, one of which is FAT32. The FAT32 format uses file allocation tables containing the location of a data cluster on the SD card and sectors of data can be written

wherever there is available space and the location of the data will be stored in the FAT. Sectors are filled with buffered data collected from the A/D converters and the FAT32 format allows for multiple files to be created on a SD card, so that many tests can be run and differentiated easily. The FAT32 format also allows for easier data extraction and analysis. (For a more in depth discussion of the FAT32 system, see Appendix A.)

Shown below in Figure 4 is a flowchart of the circuit's initializations, sampling, and shutdown.

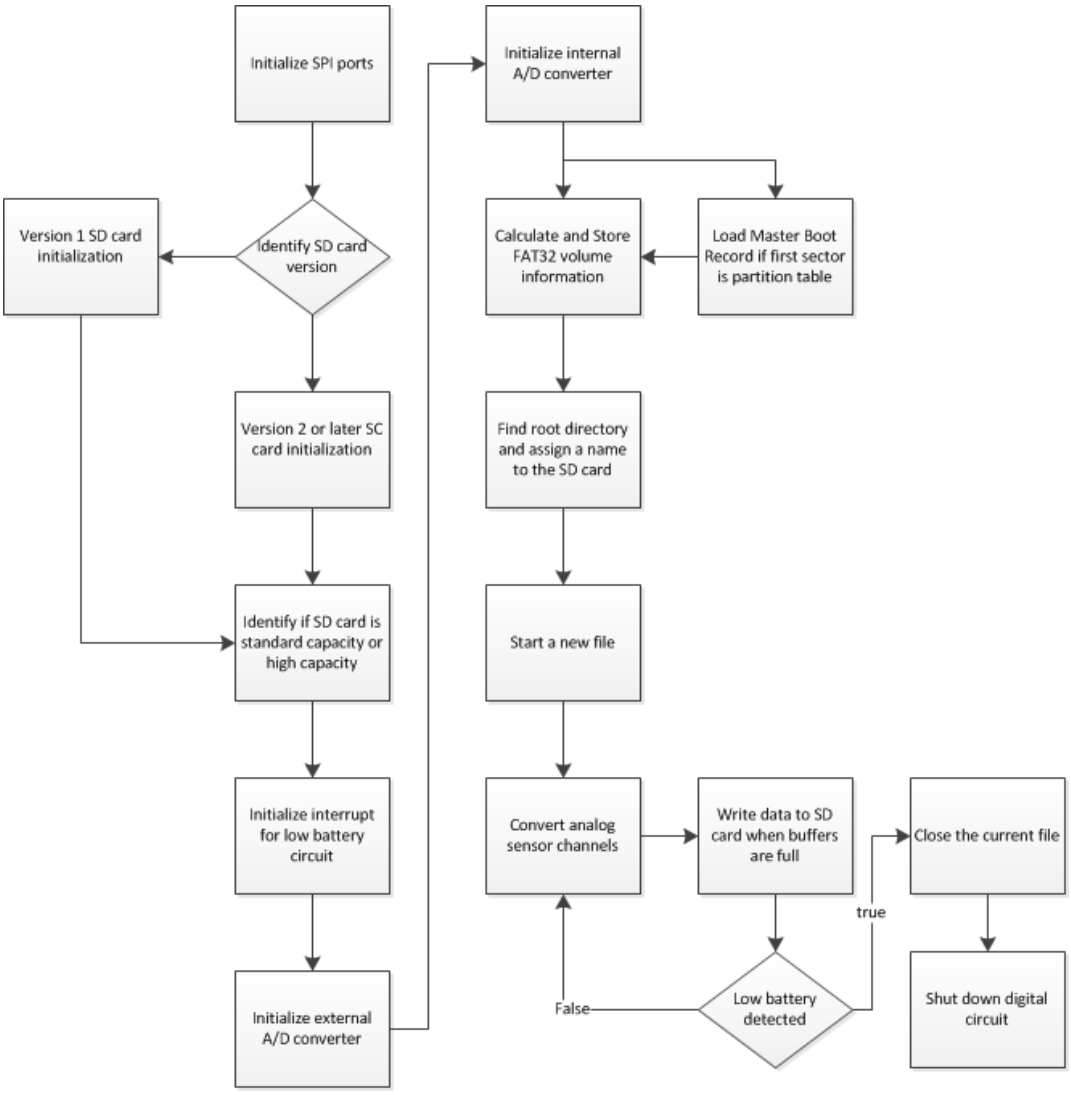

Figure 4: Flowchart of microcontroller initializations, sampling, and shutdown

2.3.2 Data Collection

After initializations are finished the microcontroller checks the SD card for files. A new file is made and the file number is incremented by one. If no files currently exist on the SD card, the first one is assigned the name “00000001.txt” or, if file “00000009.txt” exists, then file “00000010.txt” is created. If there are any errors in running the code up to this point, such as an SD card missing, the microcontroller will

sense this and throw an error causing a light emitting diode (LED) inside of the power switch to flash. The user will then know to shut the device off and to check to see if the SD card is properly installed. If there are no errors, the microcontroller begins the A/D clocks and starts the data sampling. When the A/D converters are sampled, an interrupt flag is triggered. These interrupt flags for the external A/D converters are slightly different as opposed to the internal A/D converter.

The external A/D converter is sampled at a rate determined by an output compare timer in the microcontroller. When the microcontroller requests a sample, it waits until the "busy" line on the A/D converter outputs +5 volts. When the busy line goes high, an interrupt flag is activated and a block of code is executed. The code first clears the interrupt flag then tells the A/D converter what channel to sample next, and then reads the digital value for the current channel converted. Each sample has 14 bits of data, meaning it has to be represented by 2 bytes. Once 256 samples are taken, a buffer is filled and is then written to one sector on the SD card. Writing to the SD card takes a certain amount of time; therefore, the priority levels of the interrupts have to be changed to allow the A/D converter to keep sampling while data are being written to the SD card. Also, nested interrupts must be enabled to allow an interrupt to interrupt another interrupt of lower priority while it is running a block of code. This is explained next and is visualized in Figure 5.

Sampling of the internal A/D converters is done sequentially, where each time sampling occurs, only one channel is converted. This was done to decrease the sampling rate of the internal A/D converter. The desired value for force sampling was 100 Hz per channel; however, the sampling rate could not be reduced below 908 Hz per channel

without reducing the rate of the instruction cycle of the microcontroller. The instruction cycle could not be made to run slower or data collisions could occur. Once the interrupt flag is triggered, it must be before data can be taken from the internal buffers and used to fill variable buffers. Even though the force samples are 10 bits of data, they are also represented by 2 bytes. The samples are stored in a buffer that is written to the SD card when filled. The first sample in every force buffer has an unused bit, which is used as a flag to tell the C# conversion program (Section 2.10) that it is a force sector. In addition, another unused bit in the force samples is used to signify if the event switch is depressed by the user. To keep sampling the force channels while writing, the interrupt priority levels must be adjusted to be similar to the acceleration channels.

Interrupt priority determines what interrupt to handle first if a new interrupt comes in while one is currently being serviced. The priority of the acceleration channels is always above the force channels, since the sampling rate is higher. To continue sampling force or acceleration data while writing to the SD card, their priority level must be raised above the current processor priority level, which is the priority level of the data being written, acceleration or force. When the force channels write data, the priority is raised one level but, since the acceleration base level is two levels above the force base priority level, it does not need to be changed. When the acceleration channels write, the acceleration priority level has to be above its current priority level, but so does the force priority level. To solve this, force channels are increased one priority level above the normal acceleration level and the acceleration priority is increased two above its normal level to allow it to keep sampling and to allow it to still be higher than the force priority level. A diagram of this is shown in Figure 5 below.

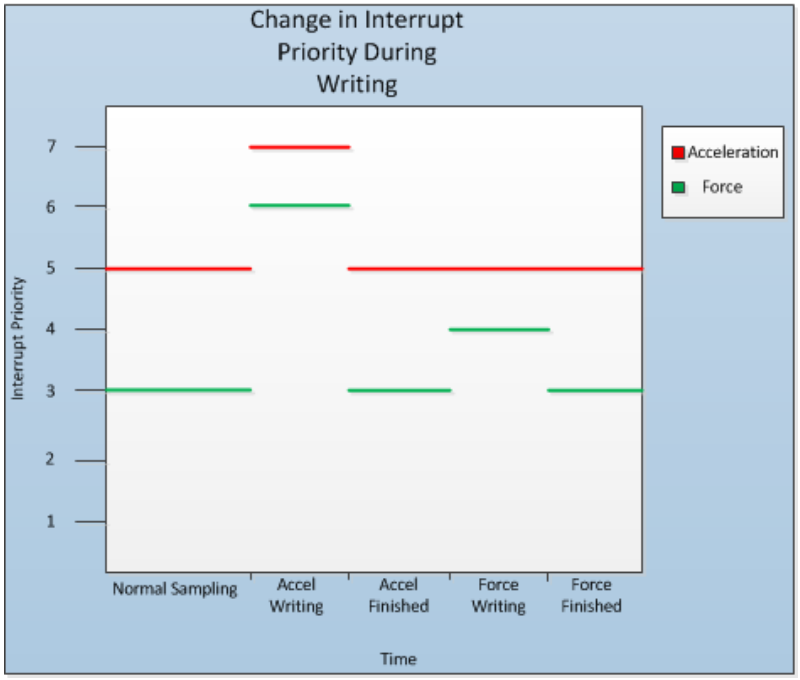

Figure 5: Diagram depicting the change in priority levels due to channels writing

2.3.3 Shutdown

The linear voltage regulators convert the battery voltage to a specified level and are powered by the batteries at all times. A shutdown pin controls if they output their specified voltage. If the shutdown pin is powered, the regulators are turned on and vice verse, if the pin is not powered. A power switch along with the microcontroller controls the shutdown pin through the use of a type of OR gate. When the power switch, the microcontroller, or both, energize the OR gate, it outputs a voltage to the shutdown pin of the regulators. When the power switch is pressed, the battery voltage is inputted to the OR gate, which turns on the regulators. This powers the microcontroller, which is programmed to output a voltage to the OR gate. When the power switch is pressed again, the OR gate is still powered by the microcontroller. A comparator, monitoring the power switch voltage, senses when the voltage is below a user set reference voltage and reacts

by outputting +5 volts. The microcontroller senses the change in the comparator output voltage using an interrupt and is told it needs to close the current file. Once the file is closed, the microcontroller stops powering the OR gate but, since the OR gate is no longer powered by the switch or the microcontroller, the voltage regulators are shut off.

If the user is not able to press the button a second time, the battery voltage may drop to a level that can no longer power the circuit. In this case, the comparator monitoring the switch voltage will sense that the battery voltage is getting low by comparing it with a user set reference voltage. As previously stated, the comparator will tell the microcontroller to close the file and stop powering the OR gate. However, the switch is still allowing the batteries to power the OR gate and the circuit will not be shut off until the batteries can no longer do this. The performance of the shutdown circuitry is visualized in Figure 6 below.

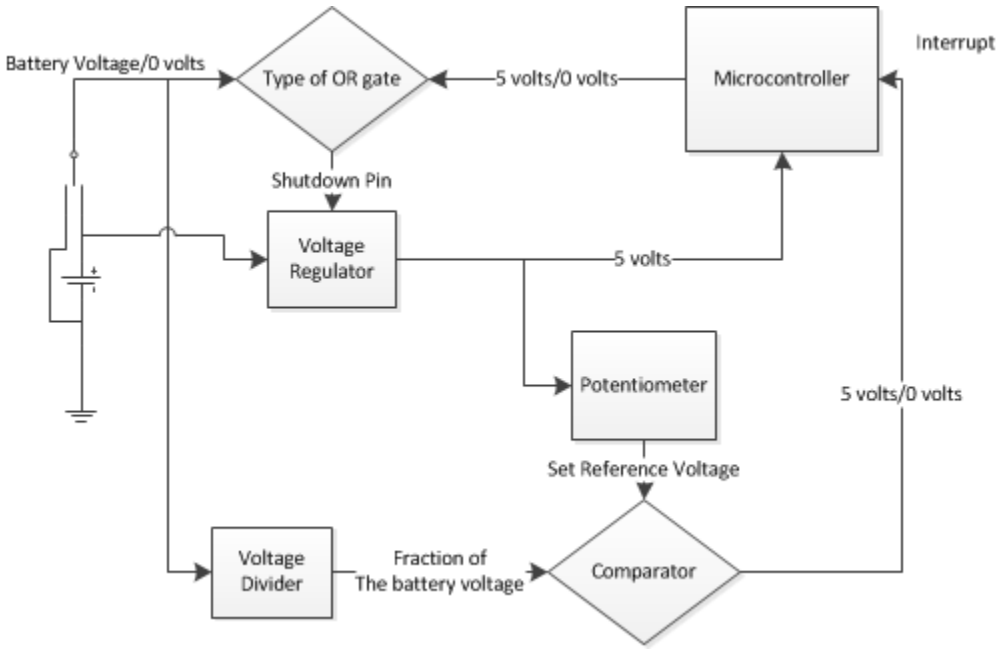

Figure 6: Low power circuitry

2.4 Data Extraction

When the user turns off the box, a file is made on the SD card with all the data from that session and each channel is written using hexadecimal values, Where two characters are used to represent one sample. The file is converted to voltage values and sorted into its correct channel file using a custom written C# program, which is initiated through MATLAB. The user specifies the location, name, output directory, and the sampling rates of the force and acceleration channels, and the voltage range measured for that channel. MATLAB then creates a file on the computer's hard drive and read by the C# program with all the information to open and write new files.

The C# program creates 17 new files, each corresponding to the filename of the data, including the designation of a force or acceleration channel and the respective channel number. The first value written to all files is the sampling rate. Next, the C#

program opens the raw data file block by block (512 bytes) and checks the first bytes most significant bit (MSB). If the MSB is a 1, then the data sector is a force block; if it is a 0, then it is an acceleration block. If it is an acceleration channel, the hexadecimal value is converted to an integer and then converted to a voltage using the voltage range specified by the MATLAB file and the number of bits of resolution hard programmed into the C# program. The voltage value is then written to its corresponding channel file. If the sector is a force sector, the second MSB is checked to determine if the event switch was pressed. If the second MSB is a 0, then a 0 is written to the event switch file (event switch is not pressed) or, if the second MSB is a 1, then a 1 is written to the event switch file (i.e., the event switch is pressed). After the event switch information is extracted, the force data in the sector is converted using the voltage range and resolution.

A MATLAB program is used to convert from voltages to force and accelerations and to analyze the data. These values are then used to calculate weighted RMS values, Fast Fourier Transforms (FFTs), or any other calculations interesting to the researcher.

2.5 Analog Front End

The accelerometers output an alternating current (AC) signal. Since the op amps used only have a supply voltage from 0 volts to 5 volts, input voltages can only be amplified to within that range. To keep voltages within range, the accelerometer front end has a voltage divider centering the signal at 2 volts and allowing for the AC signal to range between 0 volts and 4 volts because the external A/D converter can only convert values up to 4.096 volts. The accelerometers are supplied from 2 9 volt batteries in series, which means they are powered by voltages between about 14 and 18 volts. Since the voltage supplied to the accelerometers controls their maximum output, the voltage must

remain high enough to stay above the accelerometers resting voltage through out day long measurements. The accelerometers output 1 mV per m/s^2 at a resting voltage of 7 volts; for accelerations of 1000 m/s^2 a peak to peak swing of 1 volt is needed; therefore, the voltage to the sensor cannot drop below 8 volts or clipping of the signals will occur.

Using op amps, amplification circuitry adjusts the voltage levels from the sensors to the voltage range of the A/D converters. In addition to amplification, the op amps are used with resistors and capacitors to create anti-aliasing filters to prevent frequencies above the Nyquist frequency from appearing in the data and distorting it. The calculation for the Nyquist frequency (F_n) is shown in Equation 1 where F_s is the sampling frequency. For example, a sine wave with a frequency equal to the sampling rate of a device will be recorded as a direct current (DC) offset because only one data point per cycle can be recorded. This effect is called aliasing.

$$F_n = \frac{F_s}{2} \qquad \text{(Equation 1)}$$

The anti-aliasing filters remove signals above the Nyquist frequency and DC values. These are removed using a low-pass filter to remove high frequencies and a high-pass filter to remove low (DC) signals (i.e., the combination of the two filters creates a band-pass filter). Once filtering is completed, the voltage is passed through a buffer to match the impedance of the front end circuitry and the A/D converter. The analog flowchart in Figure 7 shows the steps taken to amplify, filter, and offset the acceleration channels. Currently, two tri-axial accelerometers, each having three built-in uni-axial accelerometers, and two uni-axial accelerometers will be used in the field. The tri-axial

accelerometers will be placed on each palm and the uni-axial accelerometers will be placed on each ring finger, for a total of 8 accelerometers.

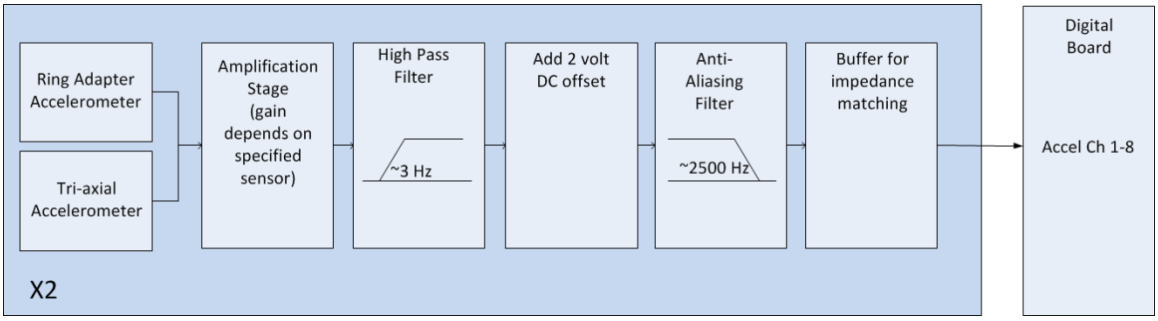

Figure 7: Accelerometer analog front end flowchart

The force sensors are supplied -5 volts by a switching regulator. When no force is applied to the sensors they will output a very high resistance causing no voltage to be outputted from the force front end. As the force sensor is compressed, the resistance is decreased creating a higher voltage outputted from the front end circuit. The force is measured from 0 to 5 volts and the gain resistor is adjusted depending on what range of force values need to be measured. Since -5 volts is supplied to the sensor and negative voltages cannot be recorded, an inverting amplifier is used to change to a positive voltage.

An anti-aliasing filter is also applied to the force channels. Since the force channels are sampled at 908 Hz, this means the Nyquist frequency is 454 Hz and any signal with a frequency above the Nyquist cannot be reconstructed. Since the force channels could not be sampled any slower than 908 Hz using the on board A/D converters, higher frequency force signals can be recorded. Oversampling is always desirable especially since it increases the resolution of the waveforms captured in the time domain. The reason why it is not desired in this device is that a low-pass filter with a

cutoff of 20 Hz is being used. After filtering takes place, a buffer is used to match the impedance from the analog front end to the impedance of the A/D converter. A diagram of the force front end is shown in Figure 8.

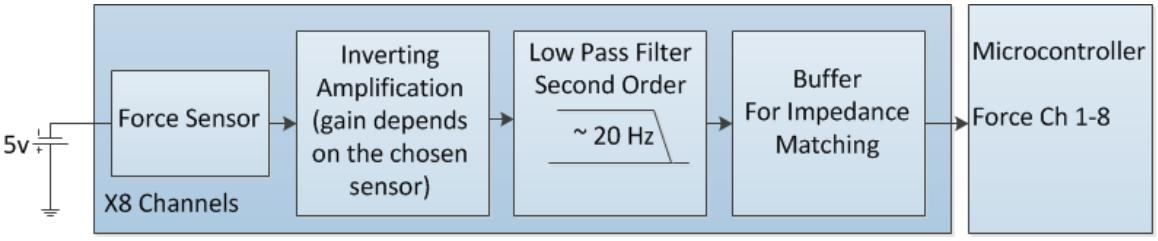

Figure 8: Force analog front end flowchart

2.7 Board Design

Once the breadboard prototype was finished, the circuit layout was designed using Altium Designer (Altium, Karlsruhe, Germany) to fit onto a printed circuit board (PCB). Since the size of the circuit would be very large using through hole components, especially considering the number of channels, the PCB had to consist of mostly surface mount components for their smaller size. Component replacement sockets were used for most IC's, which include the microcontroller, the op amps, and the external A/D converter. The problem with surface mount components is that they are mounted only on one side of the board and do not allow for traces from one side to be transferred to the other. This problem caused an increased number of traces being switched from one side of the board to the other.

The board layout was created with noise reduction in mind, where the digital part of the circuit was kept to one half of the board layout and the analog part was kept to the other half. The reason for this is to remove as much cross talk as possible between digital and analog traces. Another technique which was implemented was the use of polygon

pours for ground and power. Instead of routing the entire ground and power lines using traces, a large copper surface is placed over the entire area. This technique reduces the impedance of the power and ground lines and in turn, reduces noise. In addition, analog ground pours were separated from the digital ground pours and all pours were connected back to their corresponding regulator's ground pin in a star-like pattern.

To increase the ease of accessing the PCB, all connections from the box to the board were done using plugs from the box, which connects to male pins on the board. This allows for easy removal of the PCB for debugging or reprogramming of the microcontroller.

2.8 Testing the Device

2.8.1 Prototype Testing

Many preliminary tests were done on the breadboard prototype during design. The first test had to make sure the user can write to the SD card. This was done by creating a data block full of known values, writing it to the SD card, and then verifying the results using a program called WinHex (X-Ways AG, Cologne, Germany). This test was done using a method called single block write, which is used to initialize the SD card, FAT32, and external A/D converter. Once this was verified, multiple block write had to be tested, since it is used for actual writing to the SD card with data blocks.

Once the user could write to the SD card, the FAT 32 format was initialized. First, the device had to be turned on and turned off to make sure files appeared on the SD card. Next, the device is told to write data sectors to the opened files and then the SD card is removed from the device and opened on a computer. A text file should be seen on the

card with the data written by the user. Another test to ensure the FAT32 formatting is working properly is to write large numbers of files and to make sure they close properly. This required the device to be turned on and off several times and the verification of files on the SD card. A file on the SD card that has a size of 0 KB indicates that it was not closed properly.

The next step in creating the device was getting the A/D converter to convert values properly. This was done by having the device convert a value and then checking to see if the microcontroller obtained the correct value. This verified that the values stored in the 512-byte buffer were accurate and that the data were written to the new file properly. The interrupt priorities had to be tested and corrected to ensure the device never stops sampling (see Section 2.4.2).

Once the device was sampling properly, the A/D converters were given a known signal from a function generator and then the SD card was removed and the data were checked to verify the correct signal was obtained. This is done for all channels. During this process the event switch was also tested. Finally, comparisons of the signals allowed for testing channel synchronization in the time domain.

Once the digital circuit was working properly, the analog front end performance was confirmed by giving sensors a known value of acceleration or force, which was verified using MATLAB. Once this was finished, the device went through noise reduction testing to determine its dynamic range.

Once the device was working properly, it was tested to make sure it could capture a full work day of data. This test was performed on the bread board prototype and then

repeated for the final device. The prototype was tested using 12 AA batteries: 8 for the digital board and all twelve to power the analog board. In another test, the device was turned on and left on until the batteries ran out of power. Voltages on the board were monitored using a custom written Labview (National Instruments, Austin, TX) program that sampled and wrote to a text file. The voltages monitored were the voltage regulator input for the digital +5 volts, the voltage regulator output, the comparator output, the comparator input, the microcontroller "on/off" output, the analog battery stack voltage, the digital battery stack voltage, and the accelerometer output. The written program only allowed for four voltages to be sampled; therefore, only the voltage regulator output, the comparator output, the comparator input, and the microcontroller output were studied in detail. Current draw was recorded in another test by measuring the voltage drop across a known resistance.

To verify the Labview analysis program, the SD card being written to was completely erased leaving zeros in all data sectors. This card was then recorded to and checked to see how much data were written. By knowing the amount of data and the sampling rates, the length of time the data were written can be calculated, using Equation 2. With Equation 2, the user can also calculate how much data will be on the SD cards from how long the device ran.

$$\frac{\left(\left((Fs*Fc)+(As*Ac)\right)*2\left(\frac{Bytes}{Sam}\right)\right)*360\left(\frac{Sec}{Hr}\right)*H}{1000000000\left(\frac{Byte}{Gb}\right)} = S \qquad \text{(Equation 2)}$$

Fs= Force Sampling rate per channel
Fc= # of force channels
As= Acceleration Sampling rate per channel
Ac= # of acceleration channels
H= # of hours ran
S= Amount of data stored (in GB)

The minimum acceleration to be recorded by the device was specified as 1 m/s^2; therefore, baseline noise tests had to be performed to ensure resolution. This involved connecting an accelerometer to each channel and placing the sensor on a piece of foam on the floor (i.e., a place with minimal vibrations). Data capture was performed and the waveform was analyzed for its positive peak voltage, negative peak voltage, peak-to peak-voltage, and RMS voltage. If noise levels on a channel were not acceptable, the noise FFT waveforms were analyzed to identify the frequencies that were prevalent. These frequencies were then paired with components that were known to operate at those frequencies. Each component could then be filtered accordingly to reduce the noise in the analog signals. After filters were placed, the FFT was recreated and checked to see if attenuation of the frequency had occurred. Due to the lower resolution of the force channels, the baseline noise levels were satisfactory.

2.8.2 Fully Assembled Device Testing

Many tests on the final device were similar to the breadboard prototype tests but they were less extensive. The first test performed was to power the device using a power

supply and was performed to make sure the device was drawing the correct amount of current. Once it was verified that the current draw was normal, simple tests were made such as making sure the SD card was accumulating files, the analog front ends were amplifying and filtering properly, data collection was being performed, and error signals were working properly.

Data capture for the accelerometer channels was next tested using a calibration shaker, since the vibration output would be known. A sensor was connected to each channel and placed on top of the calibration shaker. The output of each channel was monitored by an oscilloscope and then captured using the device. The device was turned on for a time of about 30 seconds and stopped. The data were then extracted from the SD card and analyzed for magnitude and frequency. Since the gain resistor was only initially calculated and not a fixed value, the sensor magnitude would be off by a small amount. To adjust for this, whatever voltage was captured was set as 10 m/s^2 since that is the known output of the calibration shaker. For force channels, a similar procedure was done except for the use of a pinch dynamometer. Once data collection was verified, the filter characteristics had to be tested to determine amplification and attenuation at the cutoff frequencies. To accomplish this, the Dynamic Signal Analyser (DSA) (Model SR785, Stanford Research Systems, Sunnyvale, CA) was used to perform a frequency response using a swept sine wave. For the accelerometer channels, a sine wave was inputted at the sensor connection. The output was recorded after the impedance matching buffer of each channel. The range of the swept sine wave frequencies was from 3 to 10,000 Hz for acceleration channels. For force channels a swept sine could not be performed on the entire front end circuitry since the force sensors apply a resistive load; therefore, a

frequency response was only performed on the passive low-pass filters of the force channels.

Dynamic range tests had to be performed to make sure the device could record forces and accelerations of high and low enough values. Ranges of the acceleration channels were specified to be 1 to 1000 m/s^2 peak-to-peak. Since accelerations of 1000 m/s^2 peak-to-peak were unable to be simulated, device linearity had to be tested. To do this, known accelerations were given to the sensors and the voltages and corresponding accelerations were then plotted and checked for linearity. The equation of the line was obtained and the maximum acceleration was converted to a voltage and made sure it was in the range of the device. For force channels, the range specified was 0 to 100 lbs. The sensors were tested for linearity as well by using a grip dynamometer at known forces. The equation of the line was obtained and the same procedure was used to test the range of the device.

To test the absolute voltage range capabilities of the device, a harmonic distortion test was performed. This test was only able to be performed on the breadboard prototype, since the voltages inputted could damage the final device. To accomplish this test, the theoretical maximum acceleration was converted to its corresponding voltage value. The capability of the A/D Converter is 0 to 4.096 volts and the acceleration was offset to 2 volts allowing ±2 volts for an AC signal. The accelerometers being used have a sensitivity of 1 $mV/(m/s^2)$ and 1000 m/s^2 peak-to-peak maximum acceleration. A natural gain of 4 allows for specifications to be met and for the best resolution possible. To simulate this test, 500 mV peak-to-peak is supplied to the acceleration front end circuitry (500 mV corresponds to an input of 1000 m/s^2 peak-to-peak). This voltage is then applied

to the acceleration front end input and the FFT of the output signal was analyzed and checked for the percentage of harmonic distortion. The voltage was then increased incrementally until the harmonic distortion reaches 3%. Once the device output reaches 3% harmonic distortion, then this was set as the device's maximum limit.

Testing the baseline noise in the final device consisted of the same procedure used in the prototype; however, noise levels could only be captured to give a specification for the device, since limited changes could be made at this point. One final change was the battery configuration, where, due to an unexpected increase in baseline noise in the final device a new battery configuration was needed. In the previous configuration, the digital board would draw large amounts of current when writing data to the SD card, which caused a drop in voltage across the 8 battery stack powering the digital board and partially across the analog board. This drop in voltage causes a drop across the 12 battery stack and this was seen in the accelerometer output. The digital board was then changed to be powered by three 9 volt batteries (in parallel) in series with 2 AA batteries (in series). The analog board is powered by two 9 volt batteries (in parallel) in series with two 9 volt batteries (in parallel). This new configuration reduced the noise levels; however, battery drain tests had to be performed a second time because the discharge rate of the new batteries was unknown. Due to this new configuration, the battery output voltage curve had to be recorded. The device was run until the batteries were drained completely, and the relevant voltages were recorded. The voltages that were recorded were the microcontroller "on/off" output pin, the analog battery stack voltage, the digital battery stack voltage, and the comparator output voltage. Once the battery voltage curve was obtained, the voltage corresponding to 8 hours of data logging and the comparator

reference voltage were selected and set. After the comparator reference voltage was set, this test had to be performed again to make sure the current file being written to would be closed before the microcontroller lost power.

2.8.2.1 Human Testing

Human testing was done using a two handed grinding tool. Data were collected on an 8 GB high speed SD card and the device was powered by its in-field battery configuration. Two channels were captured, one for each hand, using palm adapters containing a 1 $m/s^2/mV$ accelerometer and a single Force Sensitive Resistor (FSR) sensor. The user placed the palm adapter, which was fastened using a behind the hand strap on each hand. Tape was placed on the forearm, tricep, and the upper back of the subject to make sure the sensor wires would not hinder the grinding tasks. The datalogger was attached to the users back using a holster and a belt. The completed subject configuration is shown in Figure 9 below.

Figure 9: Connected sensor configuration for human testing

Before the subject began grinding, a file was captured with the sensors connected to the calibration shaker. The subject then used a grinder to smooth a piece of steel for a duration of 20 seconds over 3 times. The grinding position is shown in Figure 10 below. The figure shows the user wearing gloves but in the data presented no gloves were used.

Figure 10: Image taken during a vibration test

After data capture the sensors and the device were removed from the subject and the force sensors were post-calibrated using a pinch grip dynamometer. The force calibration waveform is shown in Figure 11 below. The device was then opened to remove the SD card and data were extracted.

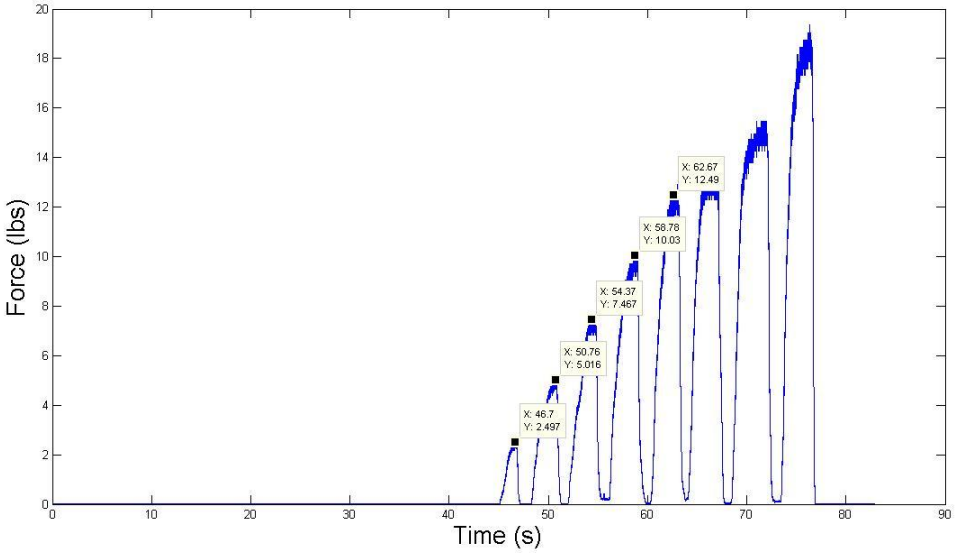

Figure 11: Force calibration waveform

3 Results

3.1 Digital Data Logging Performance

Waveform capture using a function generator was accomplished using the prototype, since direct voltages could not be applied to the final assembled device. The A/D converter was supplied with an AC signal from a function generator (Model DS345, Stanford Research Systems, Sunnyvale, CA). More specifically, the function generator supplied a sine wave with a frequency of 159.2 Hz (i.e., the frequency of the calibration shaker used in other tests), a mean voltage of 2 volts, and a peak-to-peak voltage of 3 volts. The resulting signal recorded to the SD card by the prototype is seen in Figure 12.

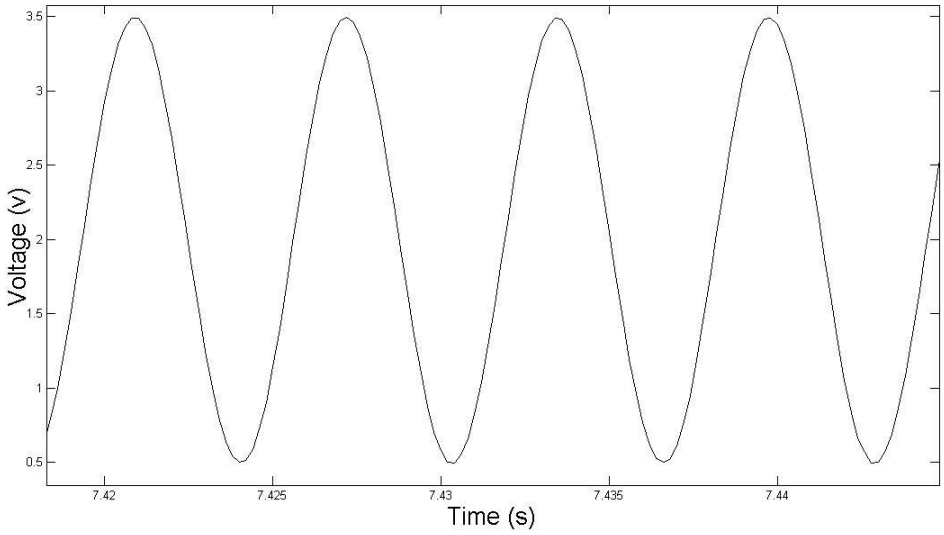

Figure 12: Snippet of the digital sine wave input test

Table 1: Sine Wave Characteristics

Signal Characteristic	Data Logger	Oscilloscope
Mean Voltage (v)	1.9985	1.99
Peak to Peak Voltage (v)	3.0115	3.07
Frequency (Hz)	159.9	159.4

The data collection represented in Figure 12 above was for a total of 30 seconds and was compared with that of an oscilloscope (TDS 3034B, Tektronix, Beaverton, OR). Calculations for the datalogger output were done using MATLAB and the frequency was calculated using an FFT. As seen in Table 1, all values were comparable to the oscilloscope values with the largest error occurring in peak-to-peak voltage, which was less than 2%.

3.2 Analog Data Logging Performance

Shown in Figure 13 is a FFT of a calibration signal. The FFT was used to measure frequencies rather than magnitudes, since the magnitude would not be seen to reach the RMS value it should have. When the waveform was analyzed in the time domain, it could be seen that the RMS value was correctly measured as shown in Figure 14. The magnitude of acceleration from the calibration shaker is 10 m/s^2 RMS and, in the figure, the peak-to-peak magnitude is about 14.15 m/s^2, which is calculated to be 10.004 m/s^2 RMS.

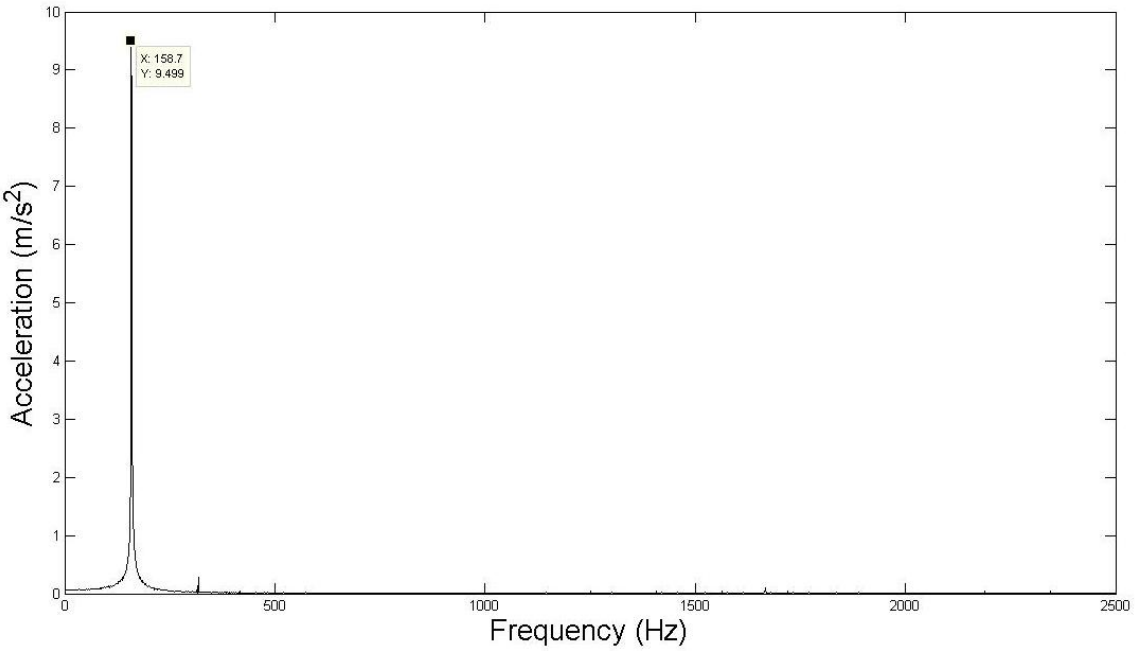

Figure 13: Recorded calibration waveform FFT

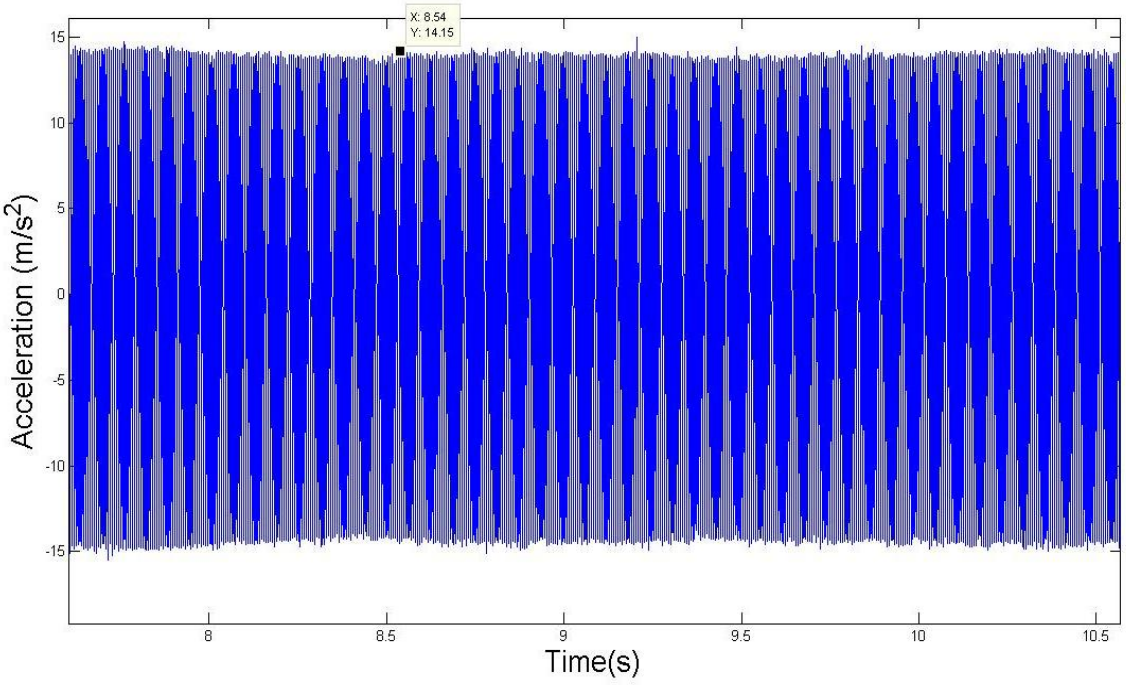

Figure 14: Calibration waveform used to calculate the FFT in Figure 13

As seen in Figure 13, the large peak is centered at 158.7 Hz, which indicates an error in frequency of 0.314%. At 317.4 Hz, a smaller peak is noticed that is a harmonic of the recorded calibration waveform.

3.2.1 Front End Gain and Filter Validation

Figure 15 below shows the frequency response of the accelerometer connected to channel 1 of the device.

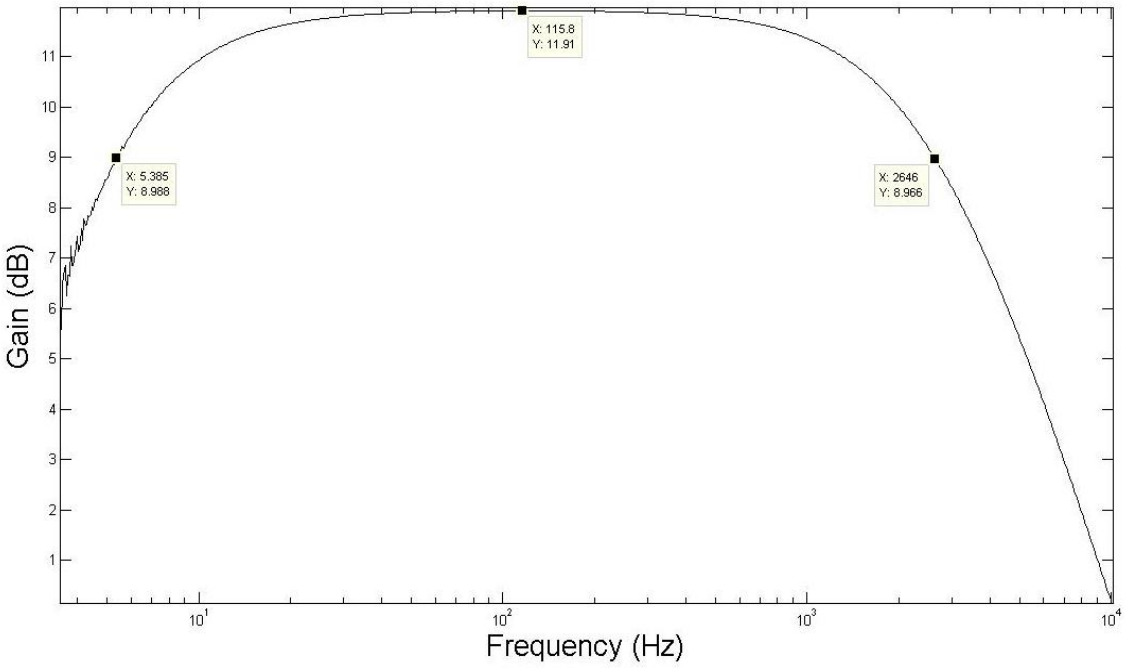

Figure 15: Bode plot of swept sine on the acceleration analog front end

It can be seen in Figure 15 that the high-pass cutoff, which is a second order filter, at 3 dB of attenuation is 5.385 Hz. The low-pass filter is a first order filter and it is shown in the figure that there is about 3 dB of attenuation at 2646 Hz. At the peak of the curve, there is about 12 dB of gain and, by using Equation 3, the natural gain is calculated to be nearly 4.

$$gain\ (dB) = 20 * log_{10}(natural\ gain) \qquad \text{(Equation 3)}$$

Figure 16 shows the Bode plot for the force analog front end and it can be seen that the frequency at 3 dB attenuation is about 11.88 Hz. This is desirable since previous tests on the force sensors have shown they are capable of recording signals above 1 KHz but for grip force measurements high frequencies are not typically of interest. Also noticed is that only attenuation is seen in the frequency response because it is a passive filter. The force front end circuitry contained no high-pass filtering, since low frequencies did not need to be filtered from these signals.

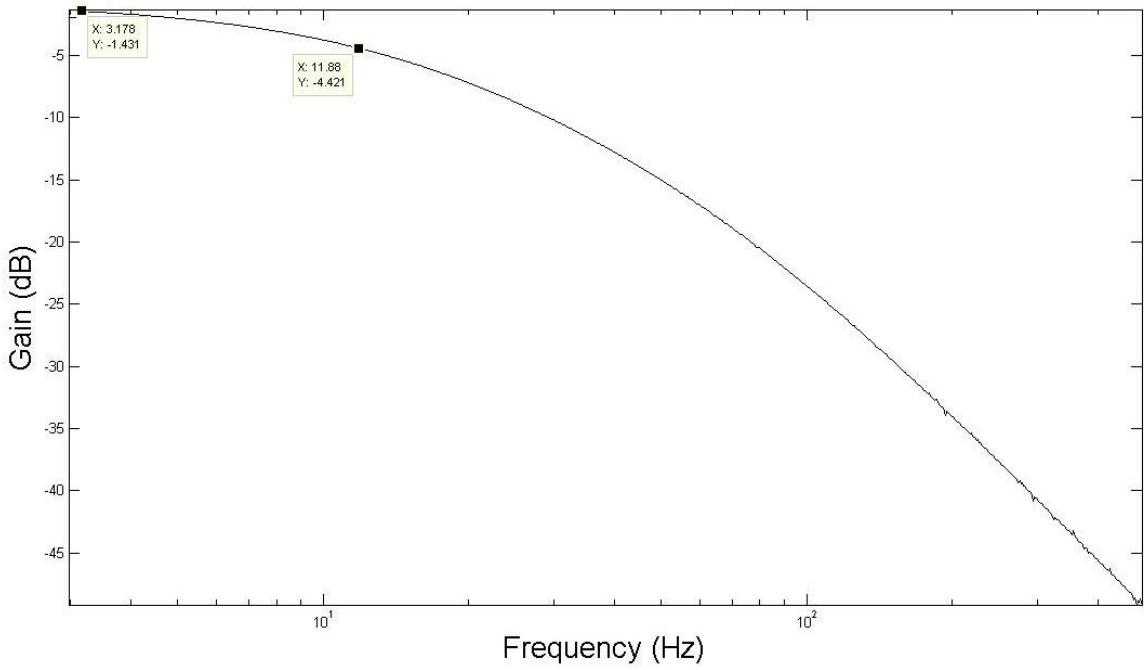

Figure 16: Bode plot of swept sine on force low-pass filter

3.2.2 Dynamic Range Test

The force range was tested using a pinch dynamometer on each channel. The grip force sensor was pressed with the dynamometer at different forces and the voltages were

compared to the force levels. The relationship was found to be linear for Flexiforce sensors, while the relationship between force and voltage for the FSR sensors had to be curve fitted (seen in Figure 11). The range of the force sensors were found to depend more on the sensor than the device (i.e., FSR sensors are only reliable up to 12 lbs. of force).

To test the dynamic range of the acceleration channels, a shaker was used to apply RMS vibration at values of 10, 20, 30, 40, 50, and 60 m/s^2. A linear equation was calculated to make sure the device could reach voltages corresponding to the specified accelerations of the device. Figure 17 shows a plot of these values.

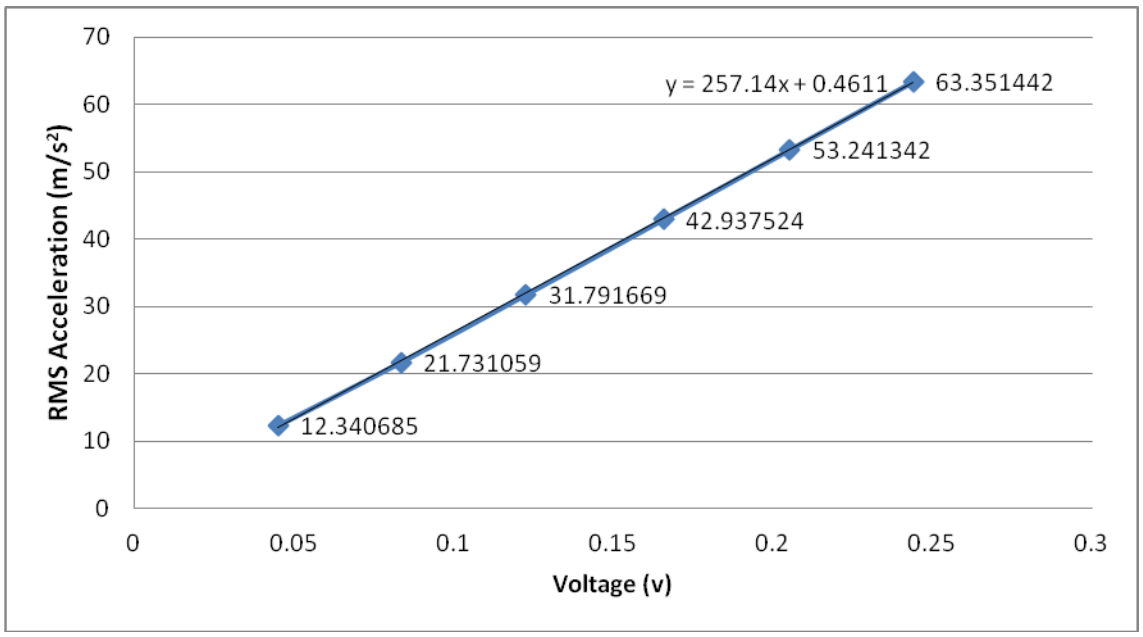

Figure 17: Linear range test results

The acceleration values in Figure 17 were recorded directly from a DSA, which are averaged, while voltage values were also recorded by the datalogger. It can be seen that the chosen values corresponded to the selected accelerations; however, since the

accelerations measured using the DSA were from an FFT, the actual acceleration values are expected to be higher (i.e., 10 m/s^2 measured by the DSA is actually about 12 m/s^2). It can be seen in Figure 17 that the acceleration analog front end is linear. Calculating for the corresponding voltage at the maximum specified acceleration results in a positive peak of 1.93 volts, which is under the maximum of 2 volts. Curve fitting Figure 17 using a second order polynomial results in the Equation 4.

$$y = 44.462*x^2 + 244.29*x + 1.1803 \qquad \text{(Equation 4)}$$

Since the voltage values are small and are squared, they become even smaller, making the non-linear portion of this equation irrelevant. This allows for the data to be represented by a linear trendline as seen in the figure.

Table 2 shows, more specifically, the results of the dynamic range test shown in Figure 17. The values captured were: positive peak (**pp**), negative peak (**np**), peak to peak (**p2p**), and root means squared (**RMS**).

Table 2: Dynamic range test results

pp (m/s^2)	np (m/s^2)	p2p (m/s^2)	RMS (m/s^2)	pp (v)	np (v)	p2p (v)	RMS (v)
9.012	-8.443	17.455	12.34069	0.031	-0.0326	0.0636	0.044965
15.6	-15.137	30.737	21.73106	0.06	-0.058	0.118	0.083426
22.377	-22.59	44.967	31.79167	0.0863	-0.0872	0.1735	0.122665
30.565	-30.167	60.732	42.93752	0.1179	-0.1164	0.2343	0.16565
37.93	-37.376	75.306	53.24134	0.146	-0.1442	0.2902	0.205171
44.166	-45.44	89.606	63.35144	0.17	-0.175	0.345	0.243915

3.2.2.1 3% Harmonic Distortion

When recording a sine wave which has an amplitude that is outside the range of the device, the maximum and minimum peaks of the sine wave will be clipped and a

clipped sine wave resembles that of a square wave. To construct a square wave at a certain frequency, many sine waves must be used at the harmonic frequencies of the base frequency; therefore, to find the maximum range of a device a harmonic distortion test is used. Clipping occurs when the device is reaching its limits and an accepted standard of harmonic distortion is typically less than 3%. Figure 18 shows the FFT of the device at 3% harmonic distortion with each harmonic clearly visible in the plot. The base frequency of the sine wave in the figure is about 159.2 Hz.

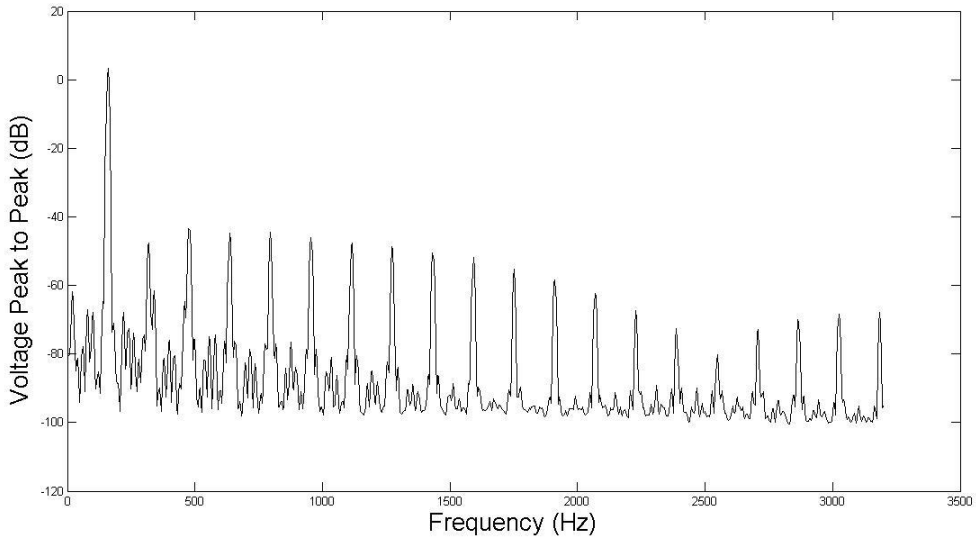

Figure 18: 3% harmonic distortion FFT of acceleration front end

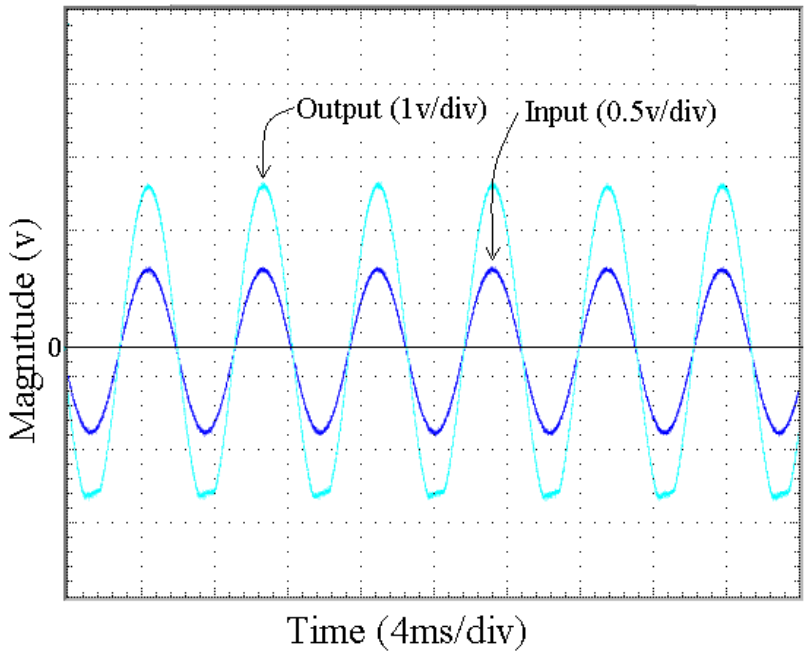

Figure 19: Oscilloscope graph of the input and output of the acceleration front end at 3% harmonic distortion

Figure 19 is a saved oscilloscope plot of the input and output channels of the acceleration front end at 3% distortion. The scale used in the figure is 0.5 volts per division for the

input and 1 volt per division for the output. The output waveform was observed to be distorted on its negative peak. The negative peak was distorted but not the positive peak because the A/D converter is capable of recording voltages from 0 to 4.096 volts and the analog front end is offset to 2 volts (i.e., the minimum capability of the device is reached before the maximum). Since the gain in the circuit is slightly below 4, the device is capable of recording above the specified acceleration (i.e., 1000 m/s^2 peak-to-peak). Once the input voltage at 3% harmonic distortion is found, the point where there is no distortion can be located and be used to find the actual maximum acceleration recordable. The input voltage before distortion was found to be 1.02 volts peak-to-peak as shown in Figure 20.

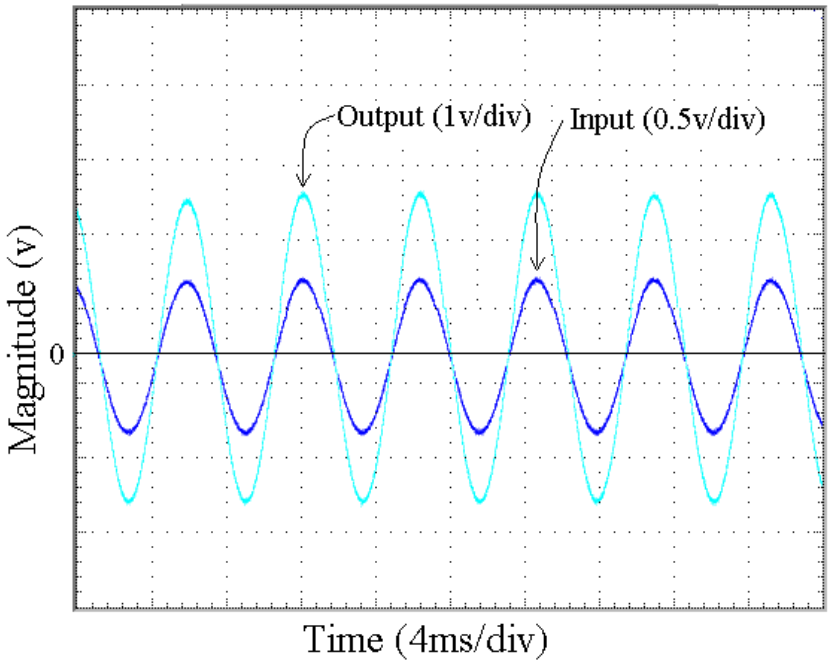

Figure 20: Waveform capture of input (channel 1) and output (channel2) before harmonic distortion. The output peak to peak voltage is about 4 volts.

Channel 1 in Figure 20 has a scale of 0.5 volts per division and channel 2 has a scale of 1 volt per division. The figure shows that the output signal is not distorted on the positive or the negative peak. The input value (i.e., 1.02 volts) was converted to m/s^2 to find the maximum acceleration, which were 1020 m/s^2 peak-to-peak for an accelerometer with a sensitivity of 1mV per m/s^2.

3.2.3 Baseline Noise Measurement

3.2.3.1 Accelerometer Noise

The noise waveforms were then analyzed to find positive peak (**pp**), negative peak (**np**), peak to peak (**p2p**), and RMS noise of the voltage and subsequent acceleration

signal. Lower noise levels increase the dynamic range of the device. In prototype noise reduction testing, positive peak noise was not an issue but negative peak noise was prevalent, due to the fact that the microcontroller writing to the SD card caused extra current draw and dropped the voltage of the battery stack. To reduce the artifact created during the writing to the SD card, different battery stacks were used for the analog and digital sections of the board. All noise levels presented in this thesis where measured after the new battery configuration was implemented. A table of noise levels for each channel is shown below in Table 3, where the channels are identified as Ch1, Ch2, etc. Note that the table contains voltage noise levels along with the resulting acceleration noise levels.

Table 3: Acceleration Baseline Noise Values

	pp (v)	**np (v)**	**p2p (v)**	**RMS (v)**	**pp (m/s^2)**	**np (m/s^2)**	**p2p (m/s^2)**	**RMS (m/s^2)**
Ch1	0.00254	-0.0018	0.00432	0.000504	0.658	-0.46	1.1187	0.131
Ch2	0.00263	-0.0025	0.0051	0.00045	0.68154	-0.6347	1.316	0.116
Ch3	0.003	-0.0033	0.00631	0.000617	0.778	-0.0858	1.636	0.16
Ch4	0.00273	0.00273	-0.0033	0.000605	0.709	-0.862	1.57	0.157
Ch5	0.00243	0.00243	-0.0030	0.000543	0.629	-0.769	1.398	0.141
Ch6	0.00214	-0.0035	0.00564	0.000486	0.5547	-0.908	1.463	0.126
Ch7	0.00264	-0.003	0.00575	0.00048	0.68464	-0.807	1.4914	0.125
Ch8	0.00283	-0.0038	0.00667	0.000762	0.7343	-0.996	1.73	0.197

Noise levels differed from channel to channel due to the placement locations of the electronic components. Since board space was limited, the analog front end components had to be placed wherever they could be fit. The peak-to-peak noise values of the acceleration channels were the absolute maximum and the absolute minimum of the waveform recorded over 4 seconds. The baseline RMS noise looks to be

less than the peak-to-peak values as seen in Figure 21. The channel presented in the figure is the channel observed to have the highest amount of noise. Note that the waveform seen in Figure 21 is not the same 4 second window used to create the data presented in Table 3.

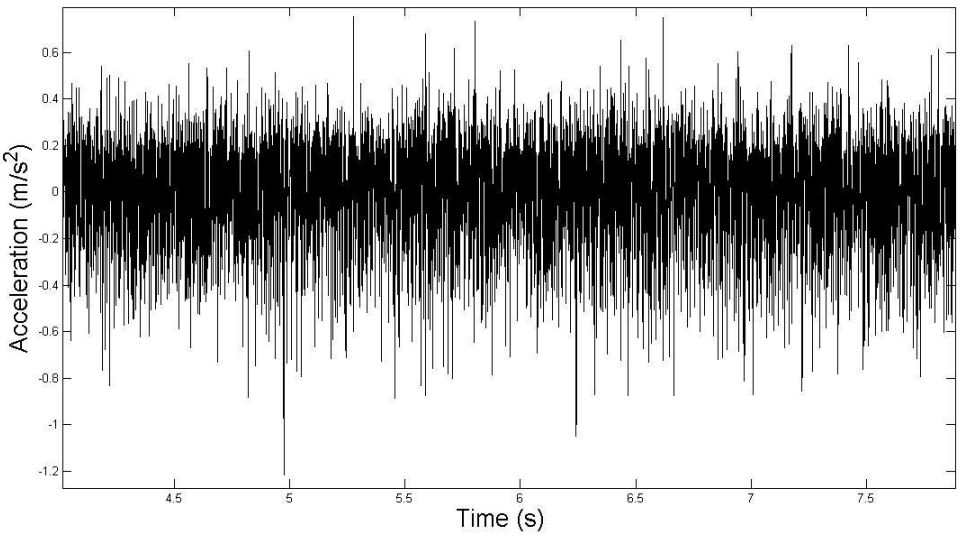

Figure 21: Baseline noise waveform of acceleration channel 8

3.2.3.2 Force Sensor Noise

The force sensors were tested for noise with the same procedure as the accelerometer sensors, where force sensors were connected to each channel, put on the floor, and recorded for a given amount of time. The channels were then separated, converted, and analyzed for the same values that were analyzed for the acceleration. For these channels, the noise levels were significantly reduced bitwise, especially since the resolution of the force channels was 1024 units while the resolution of the accelerometer channels was 16,384 units (i.e., the voltage levels may have been the same as the acceleration channels but could not be resolved by the force A/D converters). When each

channel was tested, the force sensor was pressed to make sure they were recording properly. This was important especially in channel 5 since the noise level was less than a bit which made it look as if it was not operating. Table 4 below shows the results of the force sensor noise test for all 8 channels.

Table 4: Force Sensor Baseline Noise Values

	pp (v)	np (v)	p2p (v)	RMS (v)	pp (lbs)	np (lbs)	p2p (lbs)	RMS (lbs)
Ch1	0.0049	0	0.0049	0.000142	0.0525	0	0.0525	0
Ch2	0.0049	0	0.0049	0.000192	0.0525	0	0.0525	0
Ch3	0.0049	0	0.0049	0.000406	0.0525	0	0.0525	0
Ch4	0.0049	0	0.0049	0.000969	0.0525	0	0.0525	0
Ch5	0	0	0	0	0	0	0	0
Ch6	0.0049	0	0.0049	0.0005	0.0525	0	0.0525	0
Ch7	0.0049	0	0.0049	0.000086	0.0525	0	0.0525	0
Ch8	0.0049	0	0.0049	0.00051	0.0525	0	0.0525	0

3.2.4 Device Battery Life Test

The output voltage of the battery configuration is shown in Figure 22. The current draw of the battery stack from the digital board of the device is 150 mA. The current configuration of batteries is capable of supplying 1800 mAh and can, theoretically, power the device for over 8 hours and up to 10 hours. Since the comparator takes its input from the digital board battery voltage, it was required to have the analog battery voltage last longer than the digital stack. The analog board current draw was 90 mA and the battery current rating was 1200 mAh indicating that the analog battery stack should maintain its voltage about 10% longer than the digital battery stack. It can be seen in Figure 22 that the analog battery stack (i.e., Battery 2) does maintain its voltage long enough to outlast the digital battery stack (i.e., Battery 1).

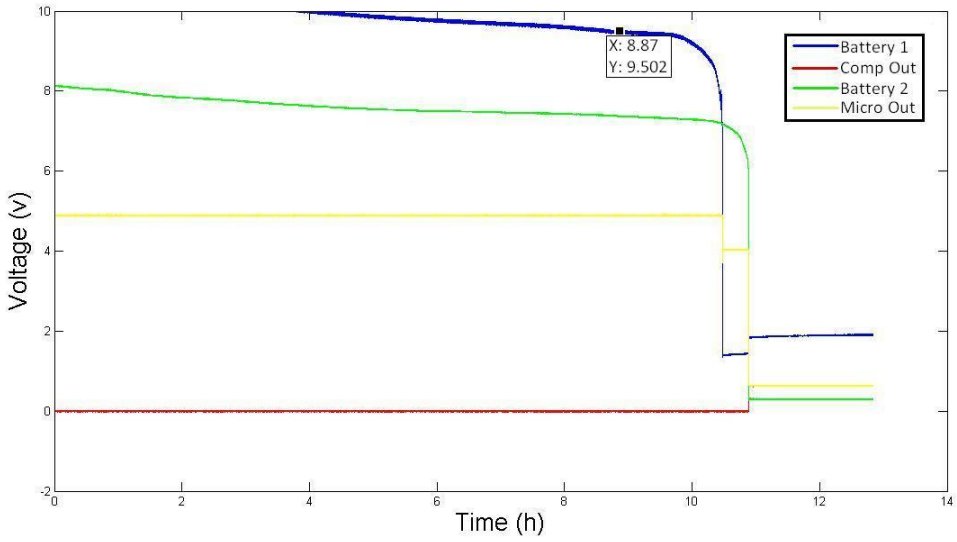

Figure 22: Battery voltage discharge curve

The voltages recorded in this test were: the digital battery stack (Battery 1), which is monitored by the comparator, the comparator output (Comp Out), which indicates when the battery voltage has reached a critical level, the analog battery stack (Battery 2), which ensures duration to make sure it is lasting long enough to power the accelerometers for an entire workday, and the microcontroller power indicator (Micro Out), which tells when the file is finished closing. Figure 22 shows that in the first four hours of the test, the device used to record voltages had a range of 0 to 10 volts. The digital battery stack voltage (Battery1) in the beginning of the test was not important and was observed to be unchanged. The analog battery stack voltage (Battery 2) was of interest and would be out of the range of the lab data collection device through out the entire test. To solve this problem, the analog battery stack voltage had to be passed through a voltage divider which divided the voltage in half to obtain its entire curve. In addition, the comparator reference voltage for this test was set to 0 volts to make sure it would not interrupt the

processor to close the file. Once the recording of the battery drain completed, curve was recorded it was analyzed to find the voltage of the digital battery stack, which allows the device to run for at least 8 hours and to have enough time to close its current file. This voltage is shown by the data point highlighted in Figure 22. Voltage was then supplied to the device by a bench-top power supply in order to find what value the comparator voltage reference should be set to but this voltage could not be calculated since a voltage divider and a low pass filter were implemented before the comparator input. After this voltage was set, the device was operated to complete battery drain and to make sure the current file was closed and that the device was turned off properly as seen in Figure 23.

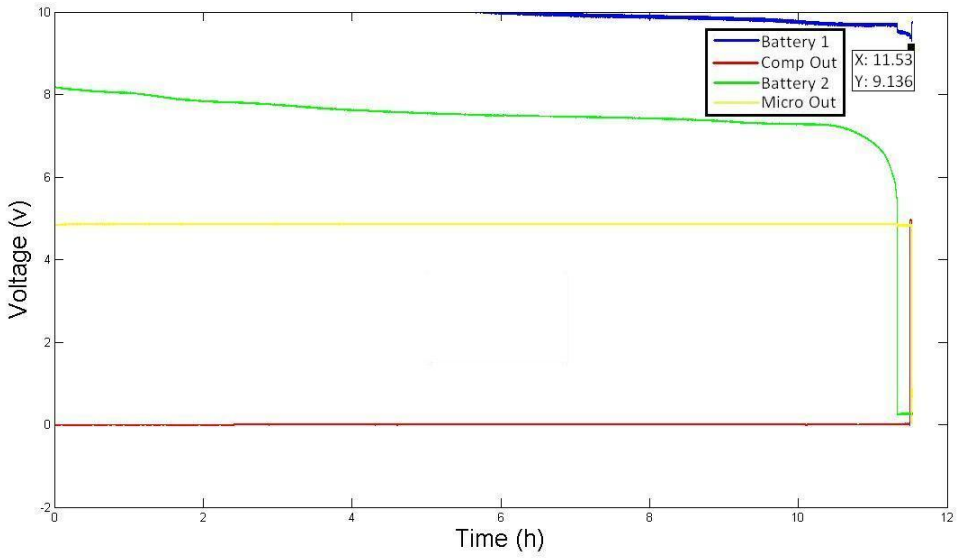

Figure 23: Battery discharge test with comparator voltage set

Figure 23 shows that the comparator output voltage (Comp Out) remained low while the device was running with enough voltage outputted from the digital battery stack (Battery 1). Once the digital battery stack voltage decreased below the set comparator reference voltage, as seen in Figure 23, the comparator output switched to +5 volts. The

change in the output from the comparator caused an interrupt flag in the microprocessor, which triggered the code to close the current file. Once the file was closed, the processor stopped outputting +5 volts, which turned the voltage regulators off (i.e., seen in Figure 23 when the Micro Out goes from 5 to 0 volts). To make sure the file was closed properly by the microprocessor, the SD card was checked for a file with the appropriate number of bytes using Equation 5.

(Equation 5)

$$\left(\left(\left(5000\frac{Samples}{Second}\right)+\left(908\frac{Samples}{Second}\right)\right)*8\ channels*2\ \frac{bytes}{sample}\right)*time(seconds)=$$

$$file\ size(bytes)$$

In Equation 5, 5000 and 908 are the sampling rates of the acceleration and force channels, respectively. The size of the file found on the SD card from the test was 3,662,111 bytes and, using Equation 5 the device was calculated to last about 10.8 hours.

3.2.5 Human Testing

Shown in Figure 24 are the results from the first vibration test with an actual human subject. As previously stated, the accelerometers and force sensors were mounted on the subject's hand. The left hand data, shown to the right of the figure, indicates about three times more acceleration than the right hand, while for the force measurements, there is about three times more force in the right hand than the left hand. It was observed that forces exerted by the right hand were similar to, or larger than the left. The accelerations were seen to be repeatedly higher in the left hand than that in the right hand.

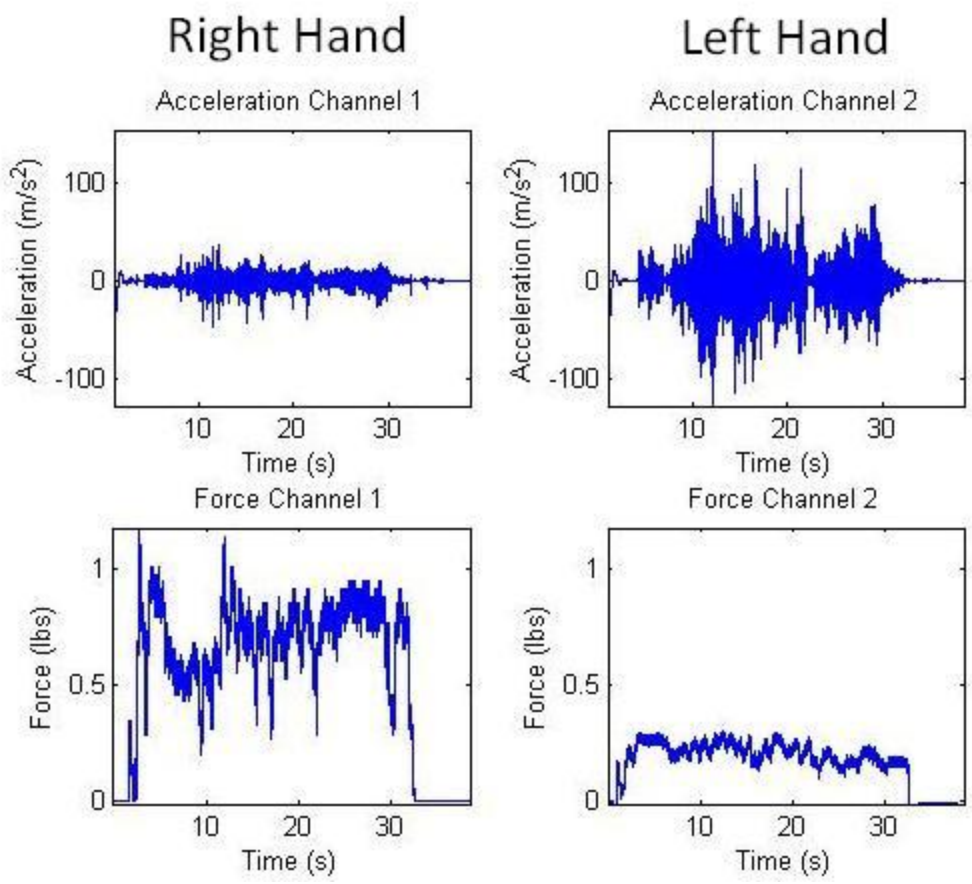

Figure 24: Results of the first grinder test showing force and acceleration curves in the right and left hand

Figure 25 shows the FFT of the acceleration waveforms for the right and left hand. The frequencies seen in each hand are similar, but the amount of acceleration is seen to be higher in the left hand. The most prominent frequencies in Figure 25 were between 50 and 150 Hz, which are within the ISO standard frequency weighting curve. According to the standard, the frequencies of vibration in the grinding tool used are considered to be harmful.

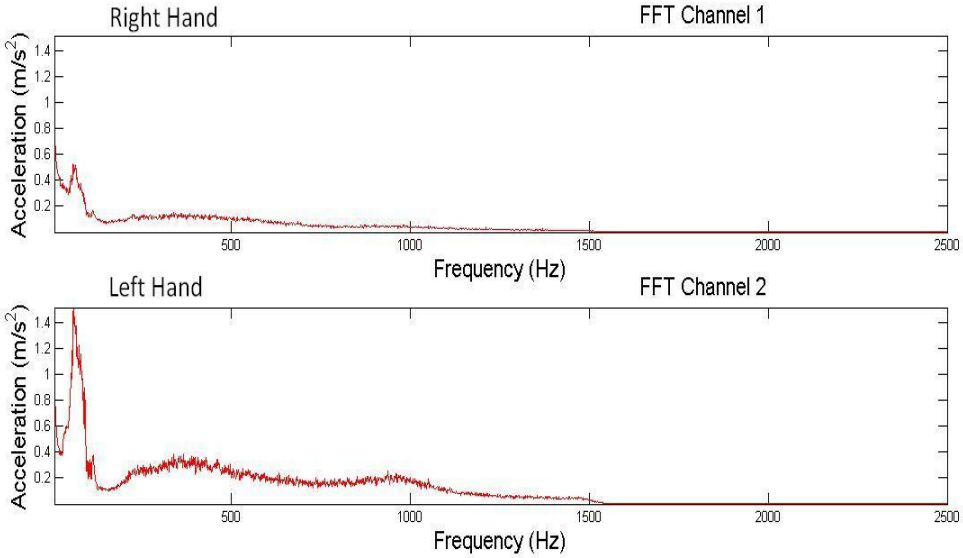

Figure 25: FFT of acceleration channels used to check if similar frequencies were seen in both hands

4 Discussion

4.1 Improvements on the Previous Device

The main reason this system improves upon other devices used for datalogging is that it allows for full waveforms to be captured for very long durations. In addition, this device is the first of its kind in the vibration datalogging field. Most devices make calculations of weighted averages and estimations of full work days using predefined standards. This was the case for the previously described VEM system, which calculated values based on 15 seconds of data per minute (see Section 1.2.3.1). The reason why raw waveforms are so important is because no data are lost in the process of logging. With the first generation VEM system, there were data limitations and the calculations showed lower results in the unfiltered data than in the filtered data. The capture of full waveforms alleviates this problem, since the waveforms can be processed and analyzed further using software in the laboratory.

The device discussed in this thesis has higher specifications than previous devices, which means a larger range of waveforms can be recorded. The sampling rate of the acceleration channels is 2 kHz higher than the EGDL system, which means higher frequency vibration signals can be recorded (i.e., signals with frequency up to 1000 Hz higher). Also, higher magnitude signals can be recorded, since the new device is specified to measure ±500 m/s^2. The higher specifications act as a safety net. If a signal with attributes above the specifications of the device is encountered, it will not be recorded properly (e.g., maxima and minima clipping or aliasing). A greater dynamic range of

acceleration magnitudes can also be captured because of the low amount of noise in the system. The device can also accommodate different acceleration and force dynamic ranges, since the gain resistors used in the accelerometer and force front end circuitry are socketed. For example, if it is known that a distribution of tools in the workplace do not produce accelerations up to the maximum range of the device, the gain resistor can be switched to reduce the range, giving the device better resolution. This was not as simple for the first generation VEM system.

The addition of more channels was also desirable for data collection. There is almost always more points of interests than there is means to collect data and, with the addition of 7 force sensor channels and 7 acceleration channels, more points on the subject can be recorded. Also, there will be the same amount of force sensors as accelerometers, which means the force applied to each accelerometer can be recorded as well as the amount of vibration at that point. This allows data to be captured on the coupling between the tool and the subject's hand at several locations.

The new high capacity SD cards are a required addition to the device as they allow for large amounts of data to be collected far beyond a normal workday. With the correct size SD card, the only component to hold back the device from capturing more than a workday's worth of data would be the battery life. Even after the battery configuration was changed the SD card could still store more data. The current battery configuration has space to add two more 9 volt batteries. Adding one 9 volt battery to the digital battery stack would cause the analog battery stack to die first, but the device would last around 16 hours. The problem with this is that the device will not close the file before the analog battery stack dies, which means there will be useless data at the end of

each file over 13.3 hours (i.e., the lifespan of the analog battery stack). To fix this, the researcher would need to remove the bad data by inspection of the waveform or even cut off data collection after a safe amount of runtime.

4.1.1 The Addition of Secured Digital Cards

Many advances in technology have been made since the design of the first generation device, including data storage capability. The previous VEM system used on-board volatile flash memory in the microcontroller and the disadvantage with this storage technique is that the data is lost once the power is discontinued. In the EGDL system, a new technique was implemented that that used on SD-card-based solid state memory. The EGDL implemented direct communication with the SD card and the microcontroller, through serial peripheral interface (SPI), allows data to be written to the SD card in no particular format, which can be read from the card using the program HxD (see Section 4.2.2). This technique requires a complete image of the card to be created, which is inefficient, especially since the image files are the full size of the SD card storage space. Also, writing to an unformatted SD card is not a very user friendly process, which is necessary since a user may not have a background in data extraction. To solve this problem in the EGDL, FAT32 formatting was used and allowed data collection to be stored to files on a removable SD card. There was one technological limitation to the EGDL system; the SD cards used at the time could only store 2GB worth of data. At the time, this was not a significant issue, since data sampling rates in the EGDL system were significantly less than the current device, which, with over 8 hours of data collection and high sampling rates, 2GBs of storage space was not enough. With advances in

technology, data storage of up to 128 GBs (i.e., SDXC) is possible with write speeds up to 45 MB/s.

4.1.1.1 Secured Digital High Capacity

When the SD card is formatted by an external computer, inserted into the device, and turned on, the microcontroller must first initialize the SPI bus for communication with the SD card; however, instead of the SD card using 5 volt digital signals like the microcontroller, it communicates using 3.3 volt digital signals. A level converter has to be used for the SD card to communicate with the microcontroller and vice versa. When the SPI is initialized, the SD card has to be identified and initialized as well. With the addition of SDHC cards to the new device, a new initialization has to be started. The microcontroller communicates with the SD card through commands and responses; therefore, the first command sent to the SD card is "command 0" which resets the card. Next, "command 8" is sent which determines the version of the SD card. The response received dictates the command that is sent next, since the initializations will change depending on the card type. If the card is a version 1 card, the initialization is carried out; however, if the card is a version 2 card or later, it has to be determined whether if the card is high capacity or not due to implications on addressing issues. Therefore, "command 58" is sent to the SD card and a response is received. In "version 1" and "version 2" standard capacity SD cards, the addressing of sectors was done using the first byte number of each sector. For example, each sector contains 512 bytes, which means sector 1 was addressed 0, sector 2 was addressed 512, and sector 3 was addressed 1024. In the high capacity SD cards, the addressing system is identified by sector number, which means sector 2 is 2 and sector 3 is 3. Addressing the sectors incorrectly could

result in an error or data can be written to the incorrect location, depending on which card is being addressed wrong.

4.1.1.2 Fat32 File Format

As previously mentioned, an unformatted SD card could be used to collect data, but it would not be user friendly and would be time consuming having to clear the SD card sectors after every use. With Fat32 formatting, the data can easily be extracted from the SD card. The basic idea behind Fat32 formatting is that the SD card is parsed into 512 byte sectors and these sectors are then combined to form clusters of data. The clusters each have a 32-bit address in a file allocation table. The address of the current cluster contains the address of the next cluster in data capture. This allows the SD card to save data wherever an available cluster is located, even if it is not adjacent to the previous cluster. Once data capture is finished, an "end of file" address is written to the last cluster's address to tell the computer how to group the data, while an address is stored in the root directory to tell the computer where the file starts. With the root directory address, the computer is able to follow data addresses until it finds the "end of file" marker allowing it to know how to split the files. In the case of many files being written, the SD card must hold information on where the next cluster is available. When the card is formatted, the FAT tables are cleared, which means the first cluster is the next available cluster; however, if a file is already stored, the FSinfo field (i.e., the location of the first available cluster's address) has to be referenced to find where the next cluster is in order to start a new file.

4.2 Design Difficulties

The difficult part of the project wasn't creating a working device, it was getting the device to meet the design specifications. Sampling rates of 40 KHz for the complete set of acceleration channels are fast and force channels could not be reduced below 908 Hz. As seen in the EGDL system, similar design constraints caused conflicts between writing speeds and file stability. Although the advances in SD technology allowed for increased write speeds from 50% to 125%, the specifications of this new device have also gone up significantly. The previous device sampled at 2 kHz per channel with ten channels for a total of 20 KHz. The current system has 8 channels sampling at 5 kHz and 8 channels sampling at 908 Hz yielding a total of 47,264 Hz, which is an increase of total sampling rate of over 136%. One technique used to organize write times was the use of write flags. These flags let the processor know when something was being written to the SD card, which caused blocks wanting to be written to wait for the current block to be finished. Once the block was finished being written, the flag was cleared and some extra time was allowed before the next block could write. Before this process was created, the system had trouble with data block collisions which caused an error in the processor. The inability to reduce the force channels sampling rate did not only cause problems with data collisions, but it caused the current draw to be higher than expected. This is one reason why the 9 volt battery configuration had to be created. The 9 volt configuration was also created to aid with noise reduction.

4.2.1 Noise Reduction

Noise in the acceleration front end circuitry was difficult to overcome with the specified dynamic range and resolution. A larger range of acceleration values means that

there will be fewer volts to represent 1 m/s^2. For example, if the voltage range is 2 volts and the acceleration range is 500 m/s^2, then 4 mV represents 1 m/s^2, which means there has to be less than 4 mV of noise to yield less than 1 m/s^2 of noise. If the voltage range is still 2 volts and the acceleration range is 200 m/s^2, 10 mV to represents 1 m/s^2, which means noise levels have to be less than 10 mV to yield less than 1 m/s^2 of noise. Obviously, the drawback to reducing the range is that higher values of acceleration cannot be captured. This may be adjusted as the device is used in different field environments, especially since the gain resistor is socketed.

One known source of generated noise originated from writing to the SD card. In the previous device when the microcontroller wrote data to the SD card, it was seen that spikes appeared in the data because the SD card draws extra current when being written to. These spikes were difficult to filter, since they were in the range of frequencies that needed to be measured. As was the case with the previous device, they could not be completely removed; however, due to different sampling rates, which results in different write speeds, the frequency of the noise was different. One way this was reduced was by changing the battery configuration for this device to use 9 volt's instead of AA's as was used in the EGDL device. An FFT is shown in Figure 26 of a baseline noise measurement after the battery configuration was changed.

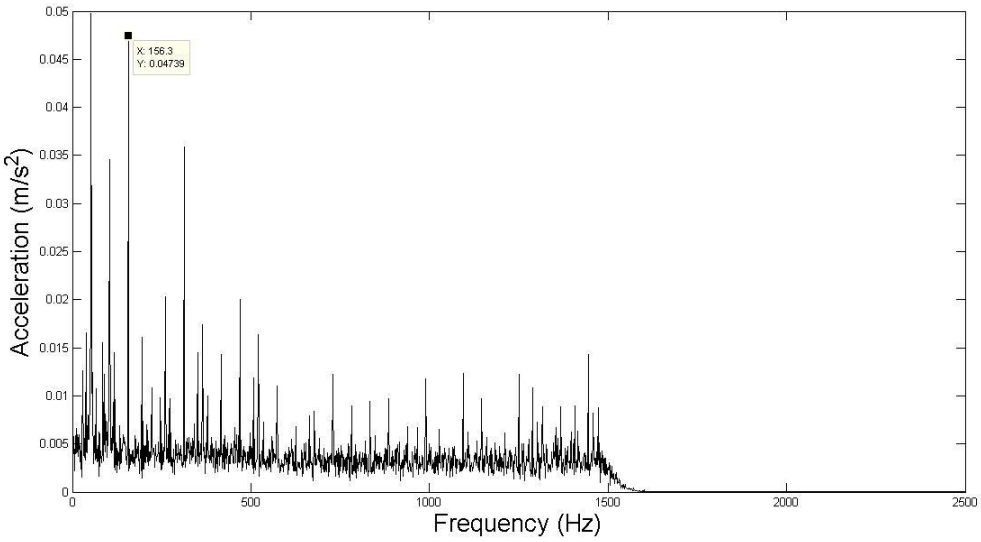

Figure 26: FFT of accelerometer baseline noise

The highlighted data in Figure 26 shows a frequency of 156.3 Hz. Although it's not the highest peak in the shown FFT, it was a frequency that was present in every noise FFT. This is the frequency is created as the microcontroller writes data to the SD card and was verified using Equation 6 below.

$$\frac{40{,}000\ \frac{Samples}{Second}}{256\ \frac{Samples}{Write}} = 156.25\ Hz \qquad \text{(Equation 6)}$$

The combined sampling rate of the acceleration channels is 40,000 samples per second and there are 256 samples per block of data. Although the writing of the acceleration channels can be seen in the FFT, the writing of the force channels cannot because the write frequency of the force channels is 28.375 Hz.

When reducing the noise of the circuit, there were a lot of theoretical assumptions that could be tested. For example, switching regulators create large amounts of noise;

therefore, the next course of action was to try to suppress the noise created by using filters, since most noise in the circuit was high frequency, low-pass filters were used. By performing an FFT on an analog channel's output, the frequency of the noise was clearly identifiable. Next, when adding a filter, the channel would be sampled again to check if the noise at that frequency was reduced. In the prototype, before noise reduction was performed, there was a switching regulator used to convert +5 to +15 volts for the accelerometer sensors. This regulator was creating large amounts of high frequency noise, so a low-pass filter was added to the output of the regulator. The difficulty was that the voltage output was high which meant high value resistors would cause a large amount of power dissipation that a quarter watt rated resistor could not dissipate. This means that the resistor value needed to be restricted to a low value. Also, large capacitor values with high voltage ratings increase in size quickly, which was a problem since circuit board space was limited. After finding the best values for the resistor and capacitor for the low-pass filter, noise was reduced but not enough to meet specifications. As a result, the switching regulator chip was eventually removed. To supply the accelerometers with their needed voltage more AA batteries were added to the prototype, which reduced the noise in the circuit dramatically; however, the battery configuration of the final device was changed to 9 volt batteries in order to reduce noise further and increase the duration of operation. Another good thing about removing the switching regulator was the fact that the current draw of the circuit was reduced about 80 mA. Since the switching regulator was powered by the analog 5 volt linear regulator, a higher current draw through this chip occurred as well. The current draw caused the analog linear regulator to become very hot, which was problematic.

Noise levels differed from channel to channel because the electronic component layout for each channel was unique, due to limited board space. A better technique of placement is to create one layout of parts for all channels and to repeat the layout for each channel so that the traces will be the same length along with the distances between components. By having similar circuit layouts the differences between channel noises would be reduced.

4.2.2 File Recovery

When the EGDL system was created, there was no means of recovering unclosed files from the SD card or corrupted files without use of the microcontroller. Additional code was used that checked for files that failed to close properly and attempted recovery to allow the data to be extracted. Recently, it has been found that by using HxD (Maël Hörz, Germany), an image of the SD card can be saved as a .txt file that contains all of the values on the SD card. This is useful in conjunction with the program RescuePRO (LC Tech, Florida, US) which can erase all data values from the SD card. A disk can, therefore, be erased completely before it is used in the field and any data written to it will be known to be from the most recent data capture session if only one capture is done. If the file is corrupted and the data are still on the SD card that signifies which cluster starts the file and ends the file, then the data can be recovered using a C# program which was written for this purpose. The only drawback is that all data spaces have to be cleared using RescuePRO before each test.

4.2.3 Device Life Test

Battery tests for the device were performed using a LabJack (LabJack Corporation, Lakewood, CO) A/D converting device, which was used in conjunction with

a custom written Labview program. There were problems with sampling rates from the LabJack and it was eventually found that the sampling rate of the Labview program was not what it should have been due to the computation time of the LabJack subcodes. Also, the Labview program could not keep the sampling rate up to the correct speed with 8 channels being sampled, causing the time domain of the calculated data to be unknown. Instead, 4 channels were sampled, which improved the Labview program but needed verification. To do this, the SD card was completely erased using Active Disk Wipe (LSoft Technologies Inc., Mississauga, Ontario) just before a battery test was performed. By checking how many sectors of data were written to the SD card, the amount of time of data capture could be calculated. In some tests, shorter times were being recorded than should have and this had to be investigated. To do this, the current draw of the circuit was monitored as a voltage using the voltage drop across a resistance (as seen in Figure 27).

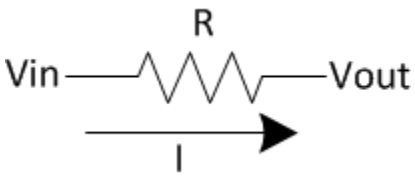

Figure 27: Simple diagram of current flowing through a resistor creating a voltage across the resistor

To measure he voltage drop, two A/D conversion channels were needed: one for Vin of the resistor and one for Vout of the resistor. The current was then calculated in software using Equation 7 below.

$$\frac{Vin - Vout}{R} = I \qquad \text{(Equation 7)}$$

R= Known resistance (<5 ohms)
Vin = Voltage before the resistor
Vout= Voltage after the resistor
I= Current flowing through the resistor

The other two channels recorded were the battery voltage and the microcontroller output. The current was observed to contain large amounts of noise that did fluctuate while the system was sampling. Without this measurement, it would have been difficult to understand why the batteries were draining as they were. In addition, the file would, at times, close early even though the Labview program would show that the device was powered for 9 hours. This was due to noise on the comparator input line from the batteries. It was noticed that some spikes would appear on the comparator line, which caused the current file to close early. To solve this problem, a low-pass filter was added between the batteries voltage divider and the comparator input.

In the second battery test (Figure 23), the analog battery stack dropped its voltage before the digital battery stack, which means data collection after this time is no good. As long as the batteries were able to last an entire work day, there is no problem. The user will be able to see when the analog battery stack voltage drops. It is when the sensors output voltage is no longer at its baseline of 2 volts indicating that the analog voltage regulator has lost its voltage. In theory, the digital battery stack should never out live the analog battery stack; however, this may occur due to issues with the batteries being used. Batteries tend to have a lifetime during which their discharge rate may vary depending on how many cycles they have gone through.

When the final assembled device was being tested, the battery test had to be completely redone due to the fact that the prototype used a different battery configuration. Wires were soldered onto test points of the final device and the same voltages were recorded as in the prototype battery test. The reason why it is important to get the battery lifetime voltage curve is because not all batteries drain the same. This was especially important for the batteries that were used. The previous batteries were rechargeable nickel metal hydride and the new batteries were rechargeable lithium ion batteries, which had never been tested in this laboratory; therefore, the characteristics of the batteries were unknown and had to be determined before they could be used.

4.3 Human Testing

The human testing shown in the results section corresponds to the user configuration in Figure 9. The subject using the grinder placed the left hand on the top handle of the grinder and the right hand on the handle of the grinder where the trigger is depressed. Analyzing the data collected by the device shows that the left hand always experienced higher levels of acceleration than the right hand.

FFT plots help show what frequencies the users are exposed to from the tools. Gathering data from multiple tools allows research groups to acquire databases full of tool signatures. This data can be correlated with what tools are found to be most dangerous and, in turn, to determine what frequencies and amount of acceleration are most dangerous. The peak frequency of the acceleration experienced from the grinder in the human test was about 80 Hz. According to the ISO standard and vibration weightings, this frequency of vibration is found to be potentially harmful.

4.4 Future Improvements

The device described in this thesis improved upon previous devices mainly because of advances in technology. Larger ranges of force and acceleration, less noise, faster sampling rates, and longer durations of time will all be possible in future upgrades to this design. One drawback may be computation time during post-capture data analysis, where analyzing data using this device from the previous ones has increased significantly since more data are being collected. If more data are being collected in future devices, data computation will increase once again.

This device does not allow multiple front end circuitries to be attached, which may be a future improvement and will allow for other types of sensors to be connected and recorded. This would be an addition to the design and could allow fewer devices to have to be made for a given series of applications. If the digital components did not have to be changed to capture data from different sensors, a reduction in the cost to produce this device will be seen, since the digital components will be common amongst all analog front ends. Board fabrication, component purchasing, and assembly will also be reduced in cost.

Finally, in the previous EGDL device a serial port was implemented to allow the user to communicate with the microcontroller using an external computer. The serial port was not implemented in this device. If it is found to be useful or even necessary, it may be incorporated into future designs or, possibly, an add-on could be made to incorporate it into the current device. Also, the battery recharge circuit may be desirable in the future because the size of the battery stack in the current device is large, which caused the user to have to remove the entire box cover to remove the batteries to be recharged.

5 Conclusion

Creating a data-logging device for a specific application involves finding the specifications that will best capture data without loss. By increasing specifications of the device (i.e., sampling rate, resolution, duration) and allowing for interchangeable front end circuitry, a high-end device can be made that can be used for multiple applications. After successfully completing the device described in this thesis, creating such a device would not be a difficult task. New components would have to be researched to meet the higher specifications but, circuit design, microcontroller programming, filter design, noise reduction, board design, and other related tasks would be similar to that of the device described in this thesis.

Previous devices used for measuring the amount of vibration to which a worker is exposed have not been able to do so with the specifications of the device described in this thesis (i.e., high sampling rates and resolution, recording duration, and large dynamic range). With previous devices, while using full day estimations and not capturing full waveforms, it is not really known how well they estimate daily vibration exposures. ISO standards, such as those described in ISO 5349, are widely accepted to present correct weightings and calculations of vibration exposure and may be seen to change in the future because of devices like the one developed in this thesis. In addition, full day, raw waveforms of vibration exposure have never been captured before. This device is seen as the first of its kind in the field of human vibration and offers a way to capture tool vibration signatures and to determine the threats they pose to workers throughout a variety of occupational settings. The information provided by this device can be used for both research and industry (e.g., producing and testing products to act as vibration

exposure control mechanisms, such as gloves). Also, it is important to measure forces applied from the subject to the tool as well as accelerations, in order to more comprehensively understand the implications of the vibration exposures. Certain brands of power tools can also be analyzed to identify harmful tools and tools can be selected that significantly improve the safety of the working environment.

6 References

[1] M. Milosevic and K. M. V. McConville, "Measurement of Vibrations and Evaluation of Protective Gloves forWork with Hand-held Power Tools in Industrial Settings," *Proceedings of the 29th Annual International Conference of the IEEE EMBS*, Aug. 2007.

[2] C. Heaver, K. S. Goonetilleke, H. Ferguson, and S. Shiralkar, "Hand–arm vibration syndrome: a common occupational hazard in industrialized countries," *Journal of Hand Surgery (European Volume)*, vol. 36, no. 5, pp. 354 -363, Jun. 2011.

[3] M. Färkkilä, I. Pyykkö, O. Korhonen, and J. Starck, "Hand grip forces during chain saw operation and vibration white finger in lumberjacks.," *British Journal of Industrial Medicine*, vol. 36, no. 4, pp. 336-341, Nov. 1979.

[4] N. J. Mansfield, *Human Response to Vibration*. CRC Press, 2005.

[5] A. Calvo and R. Deboli, "The Use of a Capacitive Sensor Matrix to Determine the Grip Forces Applied to the Olive Hand Held Harvesters," *Agricultural Engineering International: CIGR Journal*, vol. 0, no. 0, Jan. 2009.

[6] X. S. Xu et al., "The vibration transmissibility and driving-point biodynamic response of the hand exposed to vibration normal to the palm," *International Journal of Industrial Ergonomics*, vol. In Press, Corrected Proof.

[7] L. Scalise, F. Rossetti, and N. Paone, "Hand vibration: non-contact measurement of local transmissibility," *International Archives of Occupational and Environmental Health*, vol. 81, no. 1, pp. 31-40, Apr. 2007.

[8] N. J. Holter, "New method for heart studies," *Science*, vol. 134, no. 3486, pp. 1214-1220, 1961.

[9] G. Nhivekar and R. Mudholker, "Data logger and remote monitoring system for multiple parameter measurement applications," *Journal of Electrical and Electronics Engineering*, vol. 4, no. 1, pp. 139-142, 2011.

[10] Ning Liu and Zhong Su, "Research and implementation of new type multi-channel data logger," in *2010 International Conference on Computer Application and System Modeling (ICCASM)*, 2010, vol. 2, pp. V2-102-V2-105.

[11] G. Fertitta, A. D. Stefano, G. Fiscelli, and G. C. Giaconia, "A low power and high resolution data logger for submarine seismic monitoring," *Microprocessors and Microsystems*, vol. 34, no. 2-4, pp. 63-72, 2010.

[12] D. R. Peterson, A. J. Brammer, and M. G. Cherniack, "Exposure monitoring system for day-long vibration and palm force measurements," *International Journal of Industrial Ergonomics*, vol. 38, no. 9-10, pp. 676-686, 2008.

[13] E. R. Bernstein, "Portable Data Logging System for Long-Duration Field Measurement of Biomechanical Waveforms: Application to Anatomical Joint Angles and Vibration Exposures," University of Connecticut, 2008.